The Evaluation of Winds from Geopotential Height Data in the Stratosphere

WILLIAM J. RANDEL

National Center for Atmospheric Research, Boulder, CO 80307*

(Manuscript received 30 July 1986, in final form 13 May 1987)

ABSTRACT

Several methods of obtaining horizontal wind fields in the extratropical stratosphere from geopotential height data are evaluated and compared to geostrophic estimates, with focus on the poleward fluxes of momentum and heat and on the resulting Eliassen–Palm (EP) flux divergence estimates. Winds derived from a coupled iterative solution of the zonal and meridional momentum equations ("balance" winds) are proposed and tested, in addition to winds derived from linearizing these equations about the zonal mean flow ("linear" winds). Comparison of the different analysis methods are made for a general circulation model simulation of the Northern Hemisphere (NH) winter stratosphere, and for NH and Southern Hemisphere (SH) winter observational data.

The balance and linear wind estimates of poleward momentum flux are similar and substantially smaller than geostrophic values in the high-latitude stratosphere; neglect of local curvature effects is the primary cause of the geostrophic overestimate. The relative errors are larger in the southern winter stratosphere due to the stronger polar night jet. Poleward heat flux estimates are not substantially changed. Use of the improved wind fluxes results in a sizable reduction in the EP flux divergence in the high-latitude stratosphere.

Comparison with model winds suggests that the balance method is the superior analysis technique for evaluating local winds, particularly in the NH winter where local nonlinear effects can be important. Based on observed balance winds, estimates are made of the relative importance of rotational versus divergent motions in the winter stratosphere.

1. Introduction

Several recent modeling studies have suggested that the use of geostrophically evaluated winds in the extratropical stratosphere can lead to significant systematic errors in poleward fluxes of momentum and heat and in the resulting Eliassen–Palm (EP) flux divergence. Robinson (1986) showed that geostrophic winds resulted in spurious stratospheric EP flux divergence in a linear model, while a similar result was found by Boville (1987) using a general circulation model to evaluate the primitive equation and geostrophically evaluated estimates explicitly. In both of these studies, positive EP flux divergence in the high-latitude stratosphere is shown to be a spurious result derived primarily from the use of geostrophic winds in the calculations. Similar patterns of high-latitude positive EP flux divergence have been observed in the climatological studies of Geller et al. (1983, 1984) for the Northern Hemisphere (NH) winter, and Hartmann et al. (1984) and Mechoso et al. (1985) for the Southern Hemisphere (SH) winter; these observational studies were based on poleward heat and momentum fluxes evaluated geostrophically from the height fields. The aforementioned model results suggest that more accurate wind analyses may yield somewhat different results. Indeed, Elson (1986) has inferred significant ageostrophic wind components in the stratosphere from satellite observations, while Smith (1984) has noted that higher-order corrections to geostrophy can give significant improvements in comparisons with stratospheric wind observations.

The purpose of this paper is to directly compare different estimates of stratospheric wind fields and resultant higher-order quantities, derived solely from observed geopotential height data. Horizontal winds are evaluated from the height fields using 1) local geostrophic balance, 2) linearization of the zonal and meridional momentum equations about the zonal mean flow (linear winds), and 3) coupled iterative solution of the full momentum equations, less the time tendency and vertical advection terms (balance winds). Solution of the nonlinear balance equation for the winter stratosphere was studied and found to be frequently insolvable due to violation of local ellipticity constraints. Comparisons are made first within the context of a stratospheric general circulation model (GCM) simulation, where the actual model winds are available for direct comparison. Both the balance and linear wind wave fluxes exhibit relatively small differences from model "truth," as opposed to the substantial geostrophic overestimates. Balance winds are found to be considerably more accurate when evaluating local values.

Intercomparisons between the three methods are made for observational data during the NH and SH

* The National Center for Atmospheric Research is sponsored by the National Science Foundation.

winters. Results similar to the model comparisons are found for the wave momentum fluxes: substantially larger geostrophic values are observed, particularly in the SH. Small differences (on the order of 10%) are found between heat flux estimates. Detailed analyses are made for two case studies of strong wave events in the NH and SH, and climatological means are presented for January (NH) and August (SH). Balance and linear winds are used to estimate the amount of vorticity and divergence associated with planetary waves in the winter stratosphere; results reveal larger rms vorticity values by a factor of 5–10.

2. Data

a. Observational data

The observational data analyzed here are daily gridded geopotential height data from 1000–1 mb archived at NCAR. Grids below 100 mb are the 1200 UTC National Meteorological Center analyses, while data from 70–1 mb are satellite-derived geopotential thicknesses produced by the Climate Analysis Center. These are the same data as analyzed in Geller et al. (1983, 1984), Hartmann et al. (1984), and Mechoso et al. (1985). The grids are harmonically analyzed on constant latitude circles to allow analyses based on zonal wavenumber. The results presented here have been calculated using truncations at zonal wavenumber 6.

b. Model data

The model data used here are from a perpetual January simulation of the troposphere and stratosphere, based on a modified version of the NCAR Community Climate Model (CCM0). Details of the model and an extensive discussion of its climatology may be found in Boville and Randel (1986). The model geopotential and wind fields have been truncated at zonal wavenumber 6 for direct comparison with the observations.

3. Wind field analysis

a. Geostrophic and nonlinear balance winds

To obtain wind estimates from geopotential height data alone, some assumptions must be made concerning the balance between wind and height fields. A concise discussion of various balance approximations can be found in Boville (1987), while considerable details on the various levels of approximation are discussed in Gent and McWilliams (1983). Deviations from zonal symmetry in the stratosphere are primarily on the planetary scale; traditional scaling arguments for such motions (Burger, 1958; Phillips, 1963; Haltiner and Williams, 1980; Gent and McWilliams, 1983) suggest that to the lowest order, the horizontal winds are in local geostrophic balance, i.e.,

$$\mathbf{V}_g = \frac{1}{f}\mathbf{k}\times\nabla\Phi \tag{1}$$

where $f = 2\Omega \sin\phi$ is the local Coriolis parameter, ϕ latitude, $\mathbf{k}$ the unit vertical vector, and Φ is geopotential. This is the approximation made in many diagnostic analyses of the stratosphere.

If the divergent component of the horizontal wind field is assumed negligible compared to the rotational component, the nonlinear balance equation is a higher-order statement of wind–height balance (Holton, 1979; Haltiner and Williams, 1983). This approximation is most applicable to "synoptic"-scale motions; the amount of divergent versus rotational motion for planetary scales may not be small (Burger, 1958; Phillips, 1963; Haltiner and Williams, 1980; Gent and McWilliams, 1983), although measurements of their respective contributions in the stratosphere have not been made.

In spite of the fact that the results may have been of questionable applicability, solution of the nonlinear balance equation to obtain the rotational wind component was attempted for the stratospheric planetary scale motions of interest here, simply for comparison with the geostrophic winds. The nonlinear balance equation is (Holton, 1979)

$$\nabla^2\left[\Phi + \tfrac{1}{2}(\nabla\psi)^2\right] = \nabla\cdot[(f+\nabla^2\psi)\nabla\psi] \tag{2}$$

where ψ is the streamfunction for the horizontal rotational wind. For a given geopotential distribution, (2) can be inverted to obtain ψ providing the equation is elliptic. The ellipticity criterion for this equation was first discussed by Charney (1955) for the Cartesian coordinate f-plane and can be stated as a restriction on local values of the geostrophic relative vorticity:

$$\zeta_g \equiv \frac{1}{f}\nabla^2\Phi > -\frac{f}{2}. \tag{3}$$

If ζ_g is less than this value, the nonlinear balance equation (2) is hyperbolic and insolvable. In a more general context, Tribbia (1981) has discussed the realizability condition for balanced wind fields in the shallow water equations on the sphere, i.e., the conditions under which rotational balanced winds are possible for a given geopotential height field distribution. His results show that a good guide to the existence of solutions is also that the local geostrophic vorticity satisfies (3).

In this study, (2) was solved by an iterative technique starting from geostrophy. In practice, convergence of the solution was found to be closely linked with the satisfaction of (3). Unfortunately, this constraint is often violated in the winter stratosphere when large amplitude planetary waves are present; this occurs particularly often in the NH. This result suggests that the physical balance in such cases cannot be satisfied with purely rotational winds. The nonlinear balance technique for obtaining higher-order balance thus proves of little practical use in the winter stratosphere. Linear

balance winds [(2) with the nonlinear terms in ψ set to zero] were calculated and found to be quite similar to local geostrophic values; they are not discussed further here.

b. Balance winds

Gent and McWilliams (1983) suggest that the appropriate higher-order balance statements for planetary scales are the full primitive equations. A method proposed and tested here is based on iteratively solving the coupled zonal and meridional momentum equations, less the time tendency and vertical advection terms, starting from geostrophy. These solutions are termed "balance" winds. The equations are written as

$$2\Omega \sin\phi \cdot v = \frac{1}{a\cos\phi}\frac{\partial \Phi}{\partial \lambda} + \left[\frac{u}{a\cos\phi}\frac{\partial u}{\partial \lambda} + \frac{v}{a\cos\phi}\frac{\partial}{\partial \phi}(u\cos\phi)\right] \quad (4a)$$

$$2\Omega \sin\phi \cdot u = -\frac{1}{a}\frac{\partial \Phi}{\partial \phi} - \left[\frac{v}{a}\frac{\partial v}{\partial \phi} + \frac{u^2}{a}\tan\phi + \frac{u}{a\cos\phi}\frac{\partial v}{\partial \lambda}\right] \quad (4b)$$

Here u and v are the zonal and meridional velocities, λ longitude and a the earth radius. Equations (4a–b) could also be written in flux form; the resulting solutions are nearly identical.

The time tendency and vertical advection terms have been omitted for ease of solution (to make the iterative scheme two-dimensional), and also in anticipation that they may be smaller than the nonlinear (bracketed) terms in (4a)–(4b). The nonlinear terms in (4a)–(4b) are set to zero initially (yielding geostrophic winds); in each following iteration they are evaluated using winds from the previous step. A measure of the convergence of (4a)–(4b) is given by the relative wind change at each iteration, defined here as

$$\epsilon(\phi) = [\epsilon_u^2(\phi) + \epsilon_v^2(\phi)]^{1/2} \quad (5)$$

where

$$\epsilon_u(\phi) = \left[\frac{\int_0^{2\pi} d\lambda [u_n(\phi,\lambda) - u_{n-1}(\phi,\lambda)]^2}{\int_0^{2\pi} d\lambda [u_{n-1}(\phi,\lambda)]^2}\right]^{1/2}$$

is the zonal mean rms relative difference in (4b) at latitude ϕ and iteration n; a similar quantity $\epsilon_v(\phi)$ is calculated for (4a). Thorough testing of the convergence of (4a)–(4b) throughout the troposphere and stratosphere on both the model and observational data show that $\epsilon(\phi)$ typically reduces to 0.10 to 0.05 poleward of 20° latitude after 2–4 iterations for the fields truncated at zonal wavenumber 6. Although the solution is not absolutely convergent in the sense that $\epsilon(\phi)$ reduces to zero [one does not anticipate that an *exact* solution to (4a)–(4b) even exists; the true physical balance includes the terms that are omitted here], rapid nonlinear deterioration of the solution does not typically occur before accurate approximate balances can be obtained; some examples are shown below. The results shown here are produced using exactly three iterations; residuals from (4a)–(4b) using the resulting balanced winds are discussed subsequently.

Elson (1986) proposed a technique similar to the balance solution used here, based on the nonlinear momentum equations divided into zonal mean and wave components. He points out that iterative solution of the wave equations can become rapidly numerically divergent due to nonlinearities. Such behavior is not typically observed here; direct comparison for a case considered by Elson is shown later.

c. Linear winds

A much simpler estimate of higher-order balance can be made, following Robinson (1986), by linearizing (4a)–(4b) about the zonal mean wind $\bar{u}$. The resulting equations are

$$\frac{\bar{u}}{a\cos\phi}\frac{\partial u'}{\partial \lambda} - \hat{f}v' = -\frac{1}{a\cos\phi}\frac{\partial \Phi'}{\partial \lambda} \quad (6a)$$

$$\frac{\bar{u}}{a\cos\phi}\frac{\partial v'}{\partial \lambda} + \hat{f}u' = -\frac{1}{a}\frac{\partial \Phi'}{\partial \phi} \quad (6b)$$

where overbars denote zonal means and primes deviations therefrom, and

$$\hat{f} = \left[2\Omega\sin\phi - \frac{1}{a\cos\phi}\frac{\partial}{\partial\phi}(\bar{u}\cos\phi)\right]$$

$$\tilde{f} = \left(2\Omega\sin\phi + \frac{2\bar{u}}{a}\tan\phi\right).$$

These coupled equations may be solved for each zonal wavenumber to evaluate spectral components of u' and v'; the resulting wind estimates are called "linear" winds. Note that (6a)–(6b) become singular at wavenumber k as

$$\delta \equiv \frac{(\bar{u}\cdot k/a\cos\phi)^2}{(\hat{f}\tilde{f})} \to 1.$$

This is typically observed for zonal wavenumber greater than 4 in the core of the polar night jet. For the data presented here, geostrophic winds were substituted for the linear winds if $\delta > 0.5$ (the results are not sensitive to this exact value). Hitchman et al. (1987) use similar analyses, introducing more sophisticated methods of removing singularities in equatorial regions.

d. Zonal mean winds

Zonal mean geostrophic zonal winds are compared in the following sections to zonal mean balance zonal

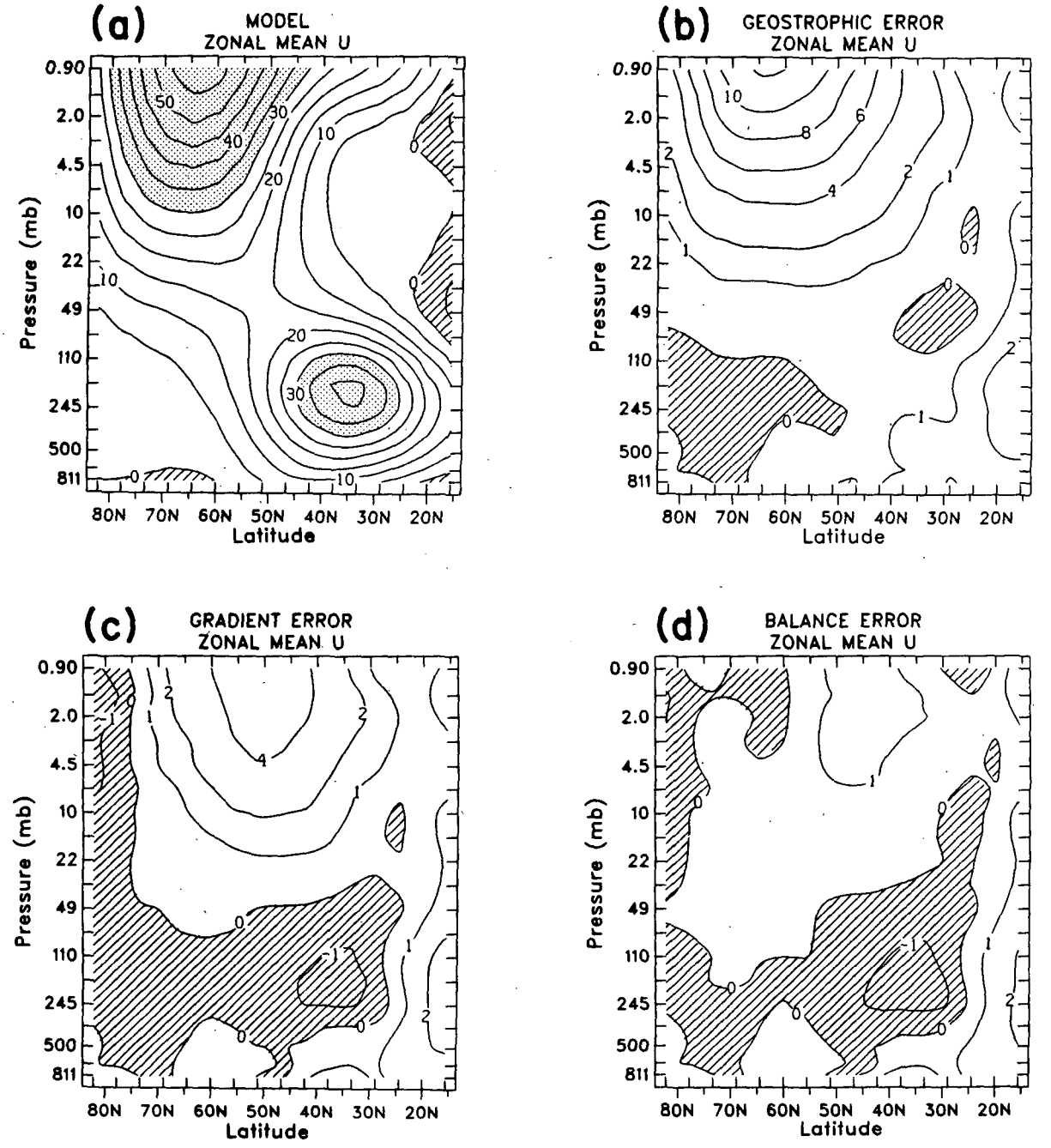

FIG. 1. (a) The 90-day average zonal mean zonal wind from model simulation, along with errors in the (b) geostrophic, (c) gradient, and (d) balance estimates of the zonal mean zonal wind. Units are m s^{-1}.

winds. In the absence of wave motions and zonal mean meridional winds, the zonal mean of (4b) reduces to a quadratic equation in $\bar{u}$:

$$\frac{\bar{u}^2}{a}\tan\phi + 2\Omega\sin\phi\bar{u} + \frac{1}{a}\frac{\partial\bar{\Phi}}{\partial\phi} = 0. \qquad (7)$$

The zonal wind resulting from (7) is sometimes called the gradient zonal mean wind; this is also calculated for the data discussed here. Equation (7) is much simpler to calculate than the zonal mean of (4b), and in practice, the resulting zonal winds usually show little difference. As discussed later, exceptions occur on some days of intense wave activity, when both geostrophic and gradient approximations exhibit large errors. The gradient zonal mean wind (7) is used for the linear wind calculations (6a)–(6b).

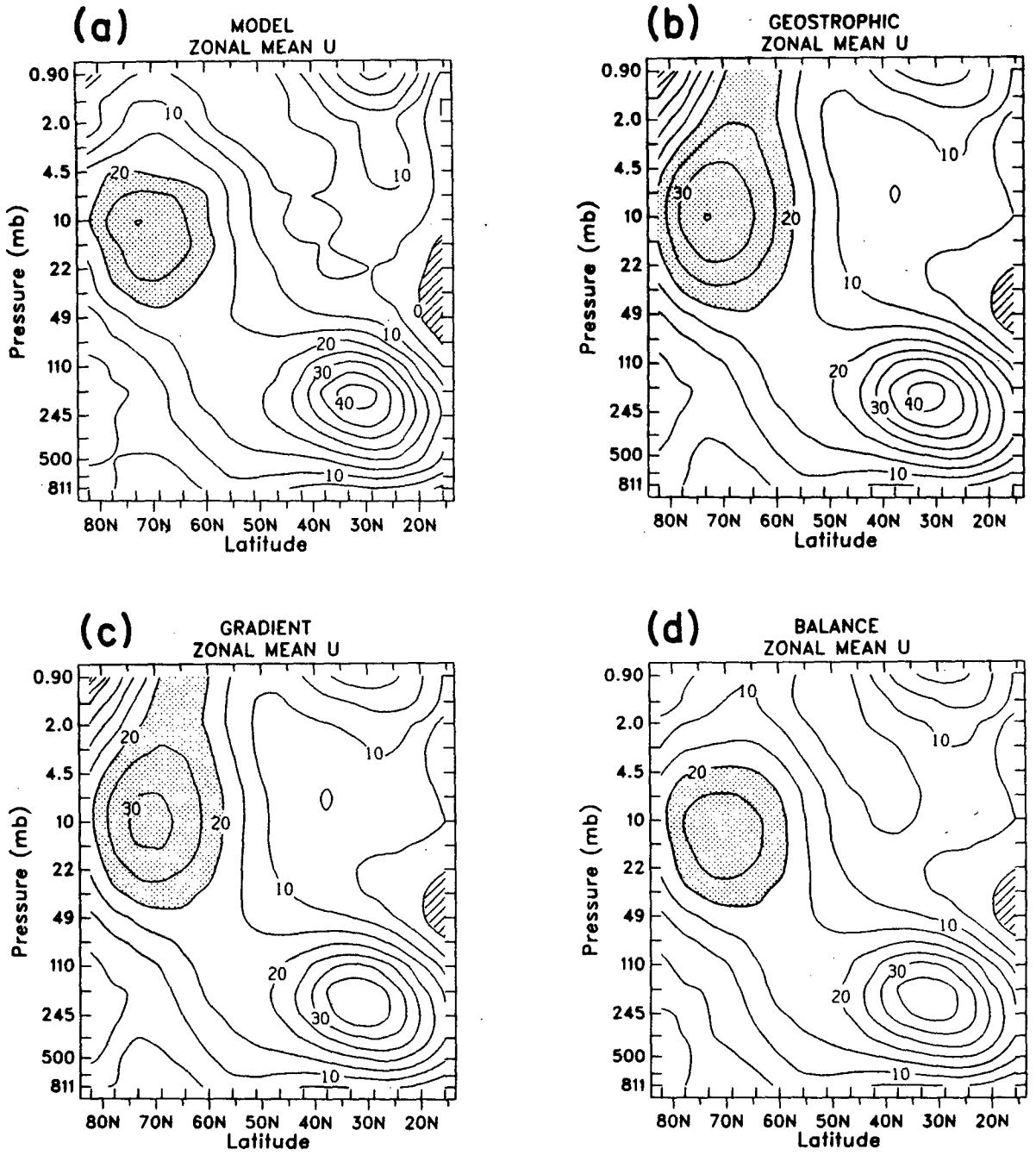

FIG. 2. (a) Instantaneous zonal mean zonal wind from model simulation, along with (b) geostrophic, (c) gradient, and (d) balance estimates, during a period of intense stratospheric wave activity. Note the substantial errors in the upper stratosphere in (b) and (c).

The balance solution winds also produce a zonal mean meridional component [from (4a)]:

$$\bar{v} = \frac{1}{2\Omega \sin\phi} \cdot \frac{1}{a\cos\phi} \overline{v \frac{\partial}{\partial\phi}(u\cos\phi)}. \qquad (8)$$

The model comparisons discussed later suggest this calculation is quite accurate in middle to high latitudes. This is one advantage of the balance winds over geostrophic or linear winds (where $\bar{v} = 0$) and may be of value for calculations such as residual meridional circulations (see, e.g., Dunkerton et al., 1981).

4. Model comparisons

The advantage of testing the wind analysis procedures on model data is that actual model winds may

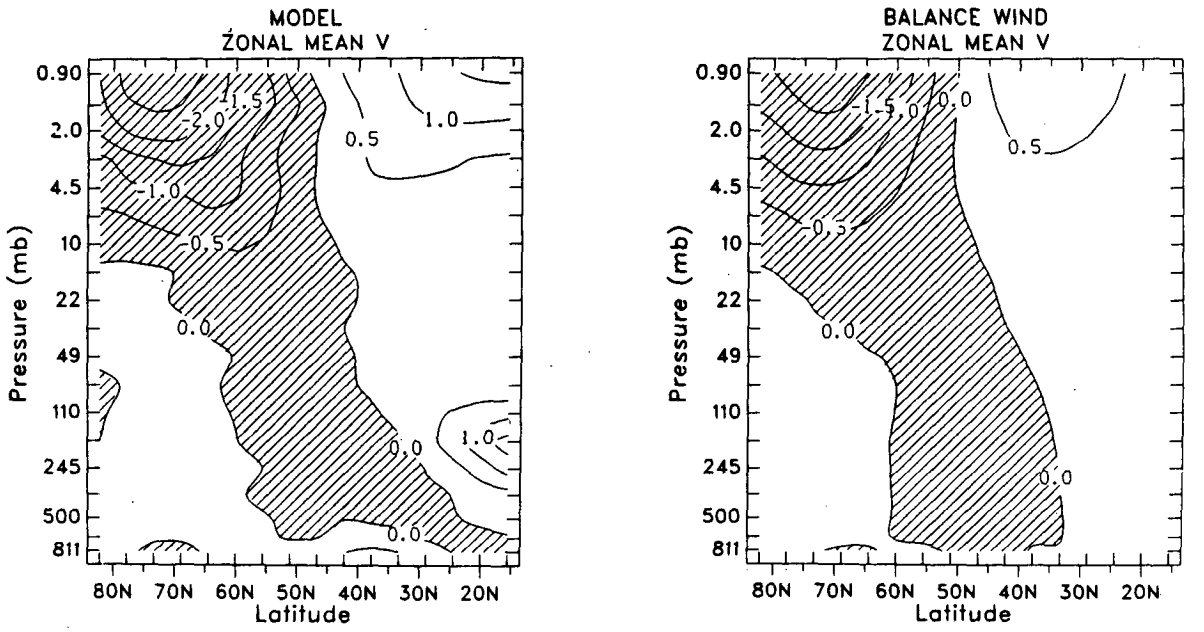

FIG. 3. Zonal mean meridional wind (left) from model simulation and (right) from balance wind estimate. Contour interval is 0.5 m s^{-1}; positive values are poleward.

be used for direct comparisons. Averages are made here over 90 days of twice-daily data, identical to the data used in Boville (1987) except where noted. Comparisons are made for zonal mean winds, zonal mean rms errors, and zonally averaged wave fluxes. The EP flux divergences are calculated using the various winds in the primitive equation expressions, neglecting terms involving the vertical velocity. One important difference in this model's climatology from NH observations is that the model stationary waves are too large in the stratosphere (Boville and Randel, 1986); this appears to be related to the perpetual January conditions under which the model was run.

a. Zonal mean winds

Figure 1 displays the 90-day average model zonal mean zonal wind, along with the *errors* resulting from estimates based on zonal mean geostrophic, gradient, and balance winds. The geostrophic wind is an overestimate by 10%–20% in the core of the polar night jet; this error is significantly reduced by using the gradient estimate (Fig. 1c). The balance wind estimate shows little difference from the model field.

Larger relative errors in the zonal mean geostrophic and gradient approximations can be found in the stratosphere on days when the wave activity is intense. Figure 2 shows the model zonal mean zonal wind, along with the three estimates, for an instantaneous time during a stratospheric warming (model day 193, discussed in Boville, 1987). In this instance, both geostrophic and gradient estimates exhibit substantial errors in the upper stratosphere (geostrophic winds are somewhat worse), whereas the balance estimate is quite accurate.

Figure 3 shows the model zonal mean meridional wind and that from the balance solution. Good agreement in the stratosphere poleward of 30°N is observed, with the balance values being underestimates by approximately 25%. Significant differences are found in low latitudes; in particular, the balance winds do not capture the northward branch of the Hadley cell in the low-latitude upper troposphere. Trenberth (1987) has used a somewhat different balance procedure to derive tropospheric zonal mean meridional winds, obtaining a more realistic structure in this region.

b. Zonal mean rms errors

In order to estimate local (zonally asymmetric) wind differences, the zonal mean rms wind errors are calculated from

$$\Delta u_{\mathrm{rms}} = \left\{ \frac{1}{2\pi} \int_0^{2\pi} [u_{\mathrm{calculated}}(\lambda) - u_{\mathrm{model}}(\lambda)]^2 \, d\lambda \right\}^{1/2},$$

where the local wind components are calculated with geostrophic, linear, or balance estimates. Zonal mean values are removed prior to this calculation. Cross sections are displayed in Fig. 4 for zonal and meridional wind components individually.

The rms zonal wind errors in the stratosphere are largest for geostrophic winds in high latitudes near the

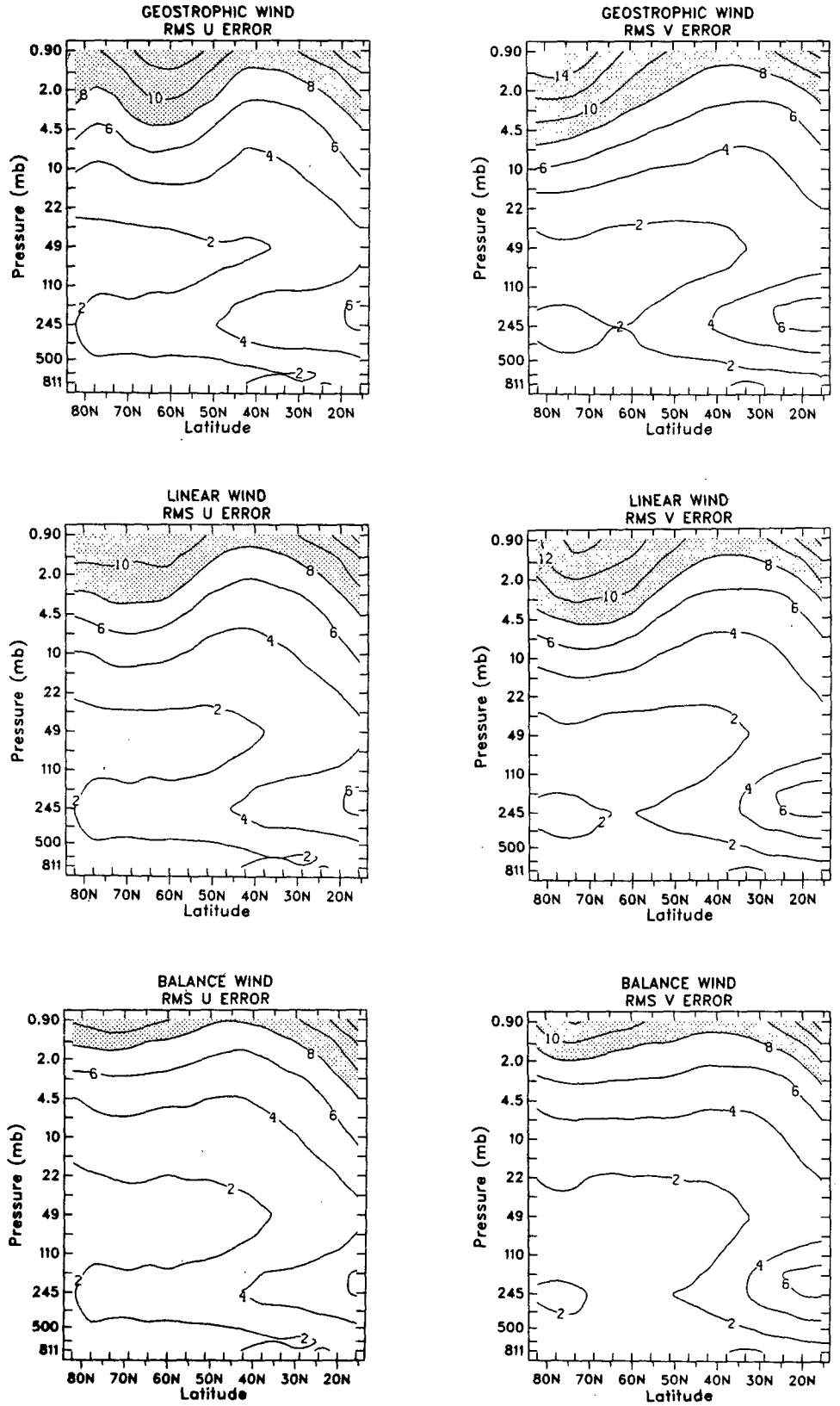

FIG. 4. Zonal mean rms differences between actual model winds and (top) geostrophic, (middle) linear, or (bottom) balance winds, for (left) zonal and (right) meridional components individually. Contour interval is 2 m s^{-1}. Zonal mean values have been removed prior to these calculations.

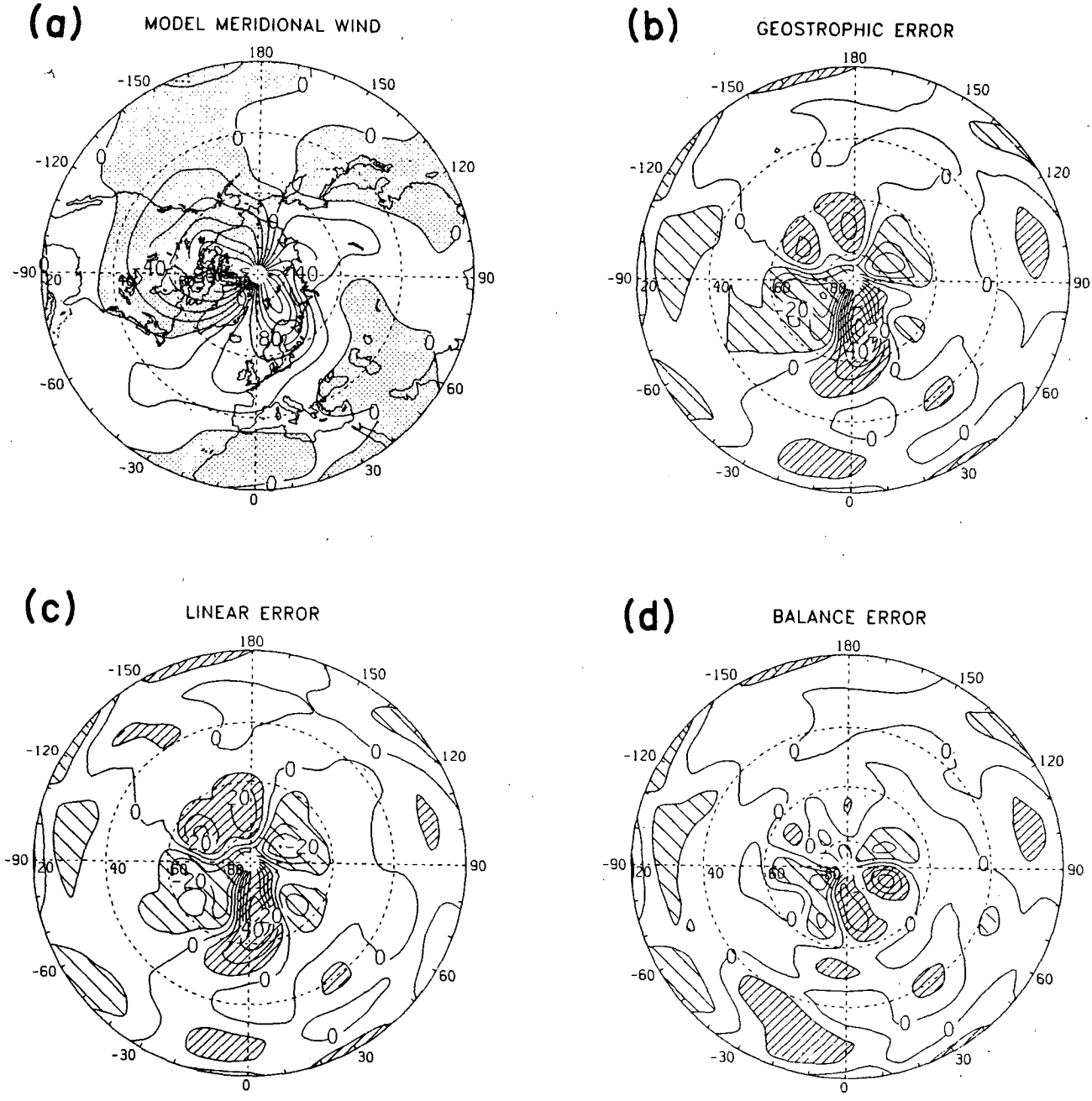

FIG. 5. (a) Model meridional wind at 1.4 mb during a day of intense wave activity (as in Fig. 2); contours of 20 m s^{-1}. Also shown are *differences* between model truth and (b) geostrophic, (c) linear and (d) balance estimates. Contours in (b)–(d) are 10 m s^{-1}, with hatched areas denoting differences greater than 10 m s^{-1}.

region of strongest zonal mean winds (cf. Fig. 1a); linear winds show only marginal improvement. The balance winds exhibit a decrease in the rms errors in this region of 40% compared to geostrophic values. The rms meridional wind errors in the high-latitude stratosphere are largest for the linear winds, roughly 10% larger than geostrophic values. The balance wind rms errors again show significant reductions, 25% smaller than geostrophy.

The improvement of local balance winds over geostrophic or linear estimates is accentuated during large amplitude wave events. Figure 5a shows the model meridional wind at 1.4 mb for a day of strong wave activity (model day 193, as in Fig. 2), along with *errors* associated with geostrophic, linear and balance estimates. The geostrophic and linear values exhibit local errors in excess of 50 m s^{-1} (Figs. 5b–c), while the balance differences show significant improvements.

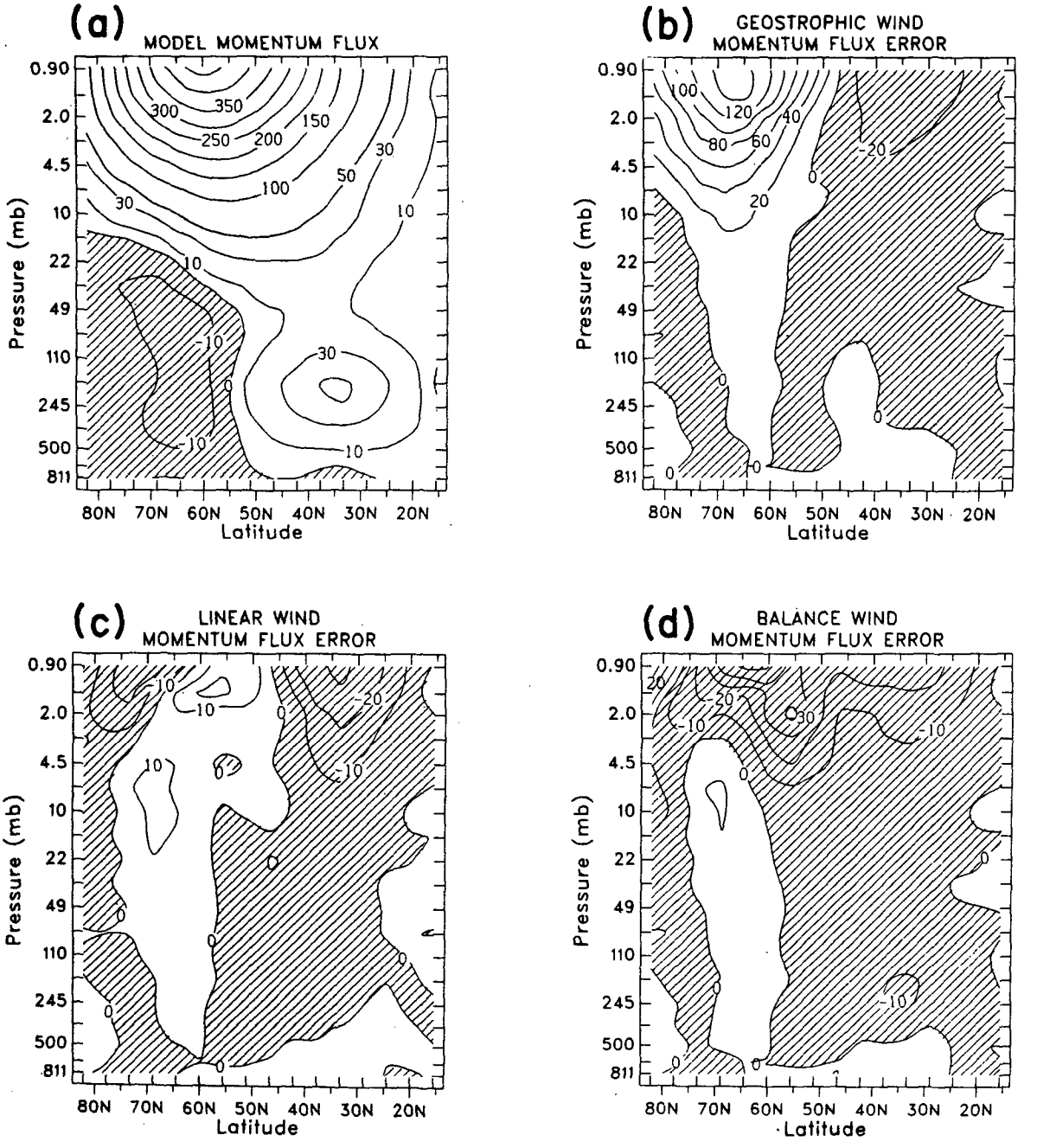

FIG. 6. (a) Model calculated poleward momentum flux, along with errors in the (b) geostrophic, (c) linear, and (d) balance wind flux estimates. Units are $m^2 s^2$.

c. Wave fluxes

Figure 6 displays the model poleward momentum flux, along with *errors* associated with evaluating the flux using geostrophic, linear, and balance winds. Geostrophic values exhibit overestimates that are greater than 40% of the true values in the high-latitude middle to upper stratosphere. In contrast, both the linear and balance wind estimates show marked improvements, with relatively small errors throughout the stratosphere.

Figure 7 shows similar comparisons for poleward heat flux calculations. Geostrophic wind estimates result in substantial errors in the high-latitude upper stratosphere, whereas linear and balance winds both give results that are in good agreement with the model flux.

Figure 8 shows an EP flux diagram incorporating wave fluxes evaluated from the true model winds, along with *errors* resulting from the use of geostrophic, linear, and balance wind flux estimates. Because of the large

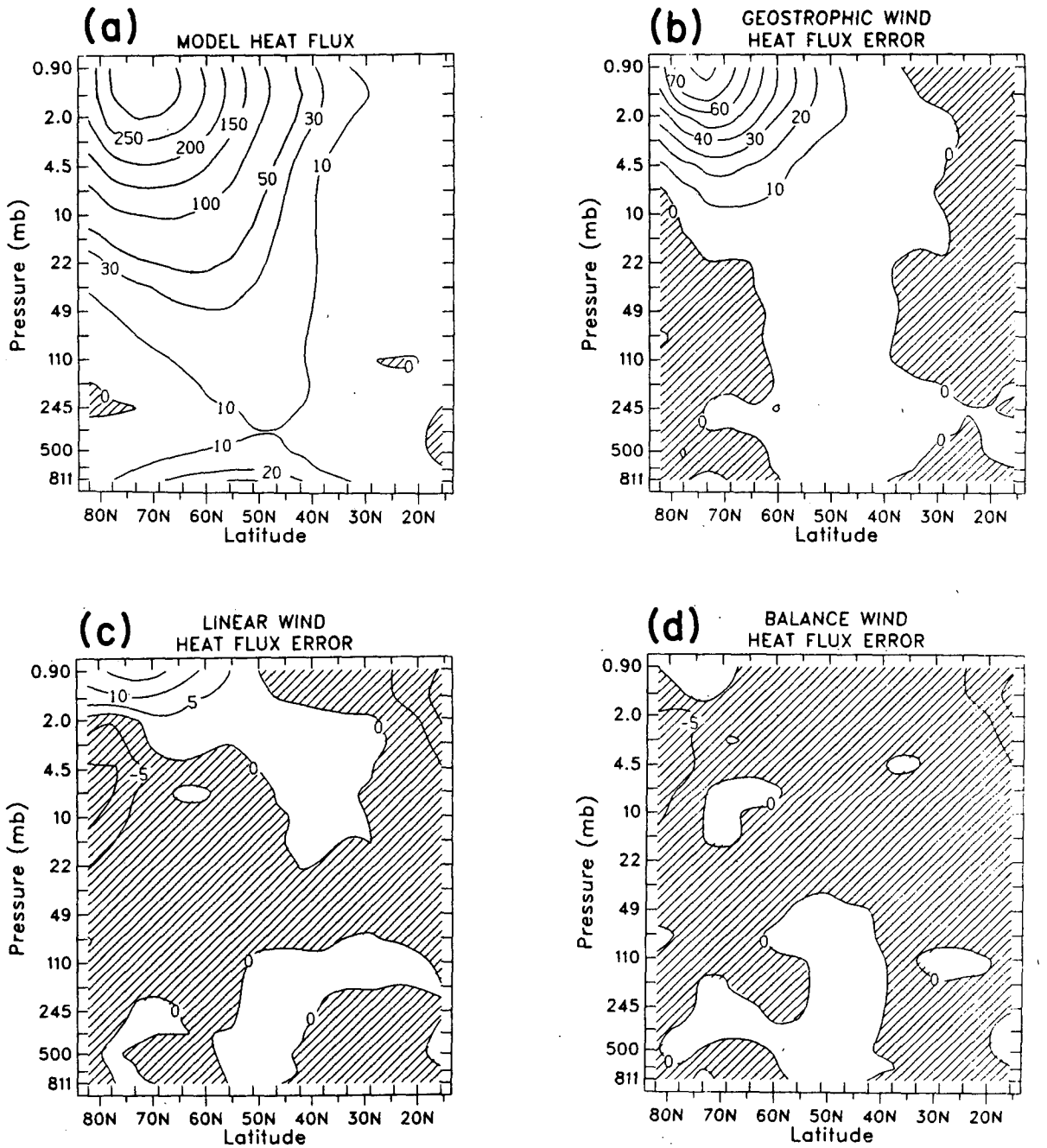

FIG. 7. As in Fig. 6 except for poleward heat flux. Units are degrees K-m s^{-1}.

errors associated with the geostrophically evaluated fluxes (Figs. 6b and 7b), the error in the geostrophic wind EP flux divergence in the high-latitude stratosphere is as large or larger than the model calculated values. In contrast, both the linear and balance wind fluxes result in significant improvements over the geostrophic estimates, although errors up to 2 m s^{-1} per day are still observed.

5. Observational data analyses

This section compares the different wind estimates applied to observed geopotential height data. Examples of the methods applied to periods of enhanced stratospheric wave activity are shown for the NH and SH, followed by comparisons for NH and SH winter climatologies.

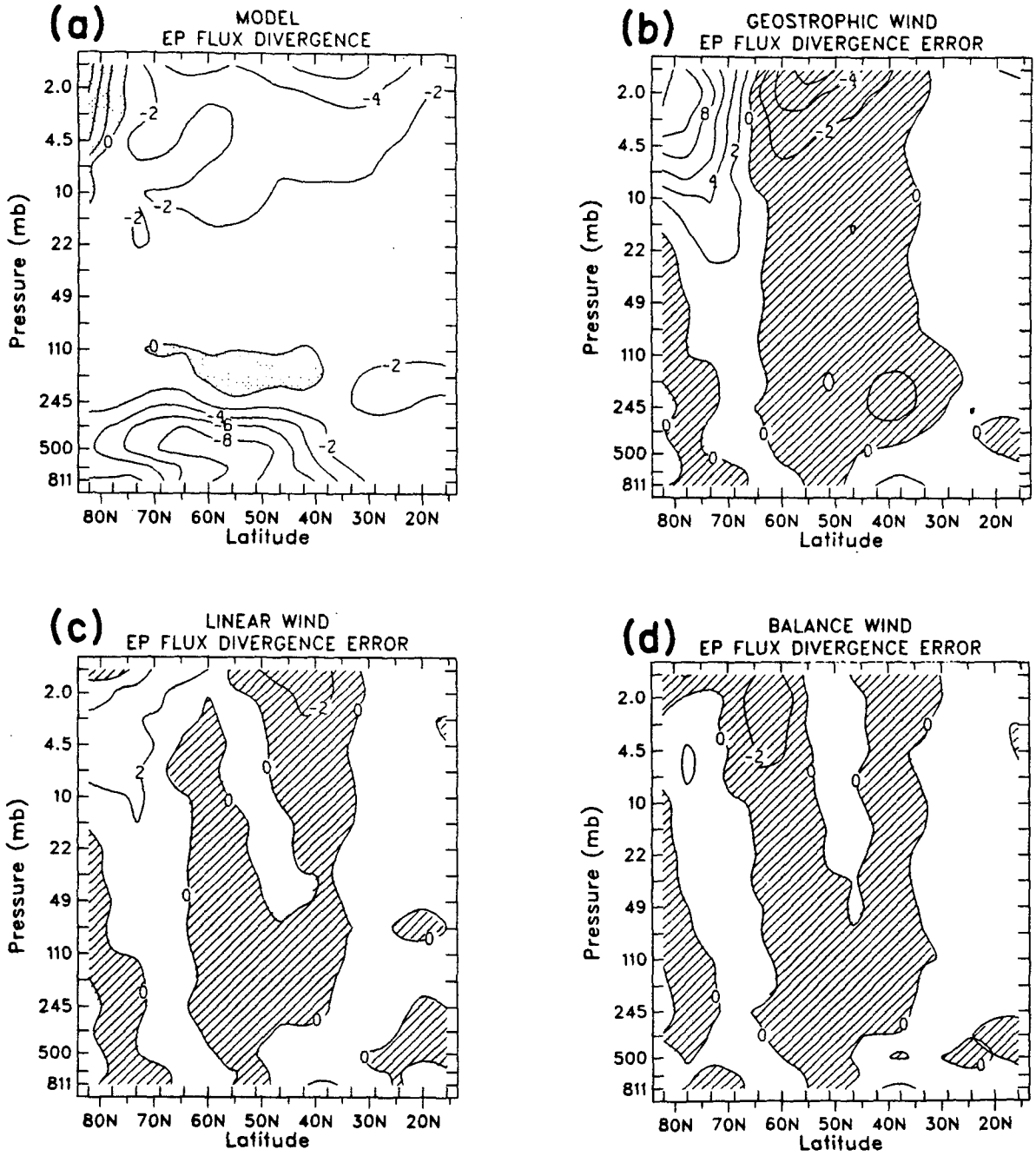

FIG. 8. As in Fig. 6 except for EP flux divergence. Contour interval is 2 m s^{-1}/day.

a. Examples

The NH case study is for 26 January 1979, the date of maximum wave amplitude during a minor stratospheric warming. Figure 9a displays the 10 mb geopotential height for this day, dominated by a strong zonal wave 1, while Fig. 9b is the quantity C, defined as the ratio of the geostrophic relative vorticity to the local Coriolis parameter:

$$C \equiv \frac{\zeta_g}{f} = \frac{1}{2\Omega \sin\phi} \cdot \frac{1}{a \cos\phi}\left[\frac{\partial v_g}{\partial \lambda} - \frac{\partial}{\partial \phi}(u_g \cos\phi)\right]. \quad (9)$$

Values of C less than -0.5 surpass the ellipticity criterion (3); large regions of $C < -0.5$ are observed in Fig. 8b, suggesting that pure rotational winds cannot be in balance with this height field.

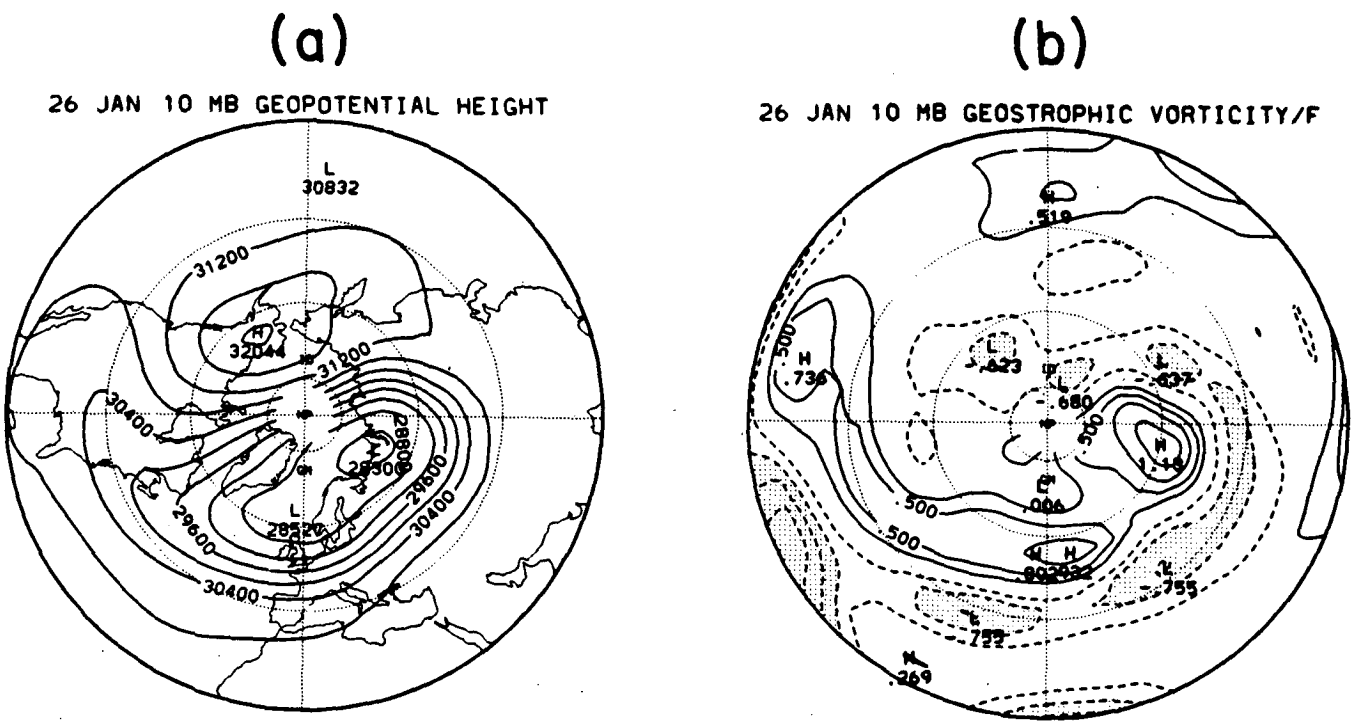

FIG. 9. NH polar stereographic projections for 26 January 1979 of the (a) 10 mb geopotential height (contour interval of 400 gpm) and (b) ratio of the geostrophic relative vorticity to local Coriolis parameter (contour interval of 0.25). Shaded values (less than −0.5) in (b) surpass the nonlinear balance ellipticity criterion (Eq. 3). In this and the following polar plots the outer latitude is 20°.

Figure 10 displays the convergent behavior of the iterative balance technique by plotting the area weighted latitudinal average of $\epsilon(\phi)$ (Eq. 5) versus iteration number. The relative difference drops to 0.05–0.10 after several iterations and remains fairly constant for several steps. The solution for this day begins to deteriorate following the sixth iteration. Figure 10 also shows a similar plot for 12 February 1979, a "rapidly numerically divergent" case discussed by Elson (1986). Here the balance scheme is found to be well behaved up to the sixth iteration; likewise, for 23 February 1979 (also shown in Fig. 10), the peak of the major warming during this year.

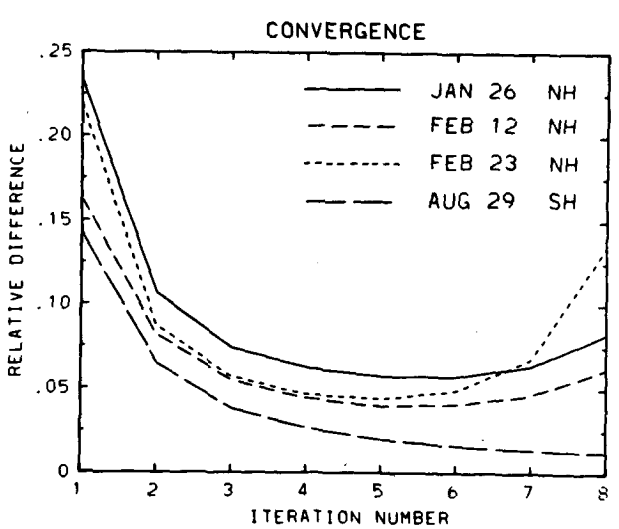

FIG. 10. Area weighted latitudinal average of the relative difference in balance wind estimates (Eq. 5) versus iteration number, for several examples discussed in the text.

Figure 11 shows the 10 mb geostrophic zonal and meridional wind estimates, along with the linear and balance wind estimates displayed as differences from geostrophic values. Similar overall patterns in the linear and balance wind difference fields are observed, showing that geostrophic balance generally overestimates local wind values, particularly in regions of strong local streamline curvature (cf. Fig. 9a). For this example, balance winds show substantially larger local differences than linear winds, primarily because the zonal mean wind (from which the linear winds are calculated) is substantially different from local zonal wind values.

The degree to which the iteratively derived balance winds satisfy (4a)–(4b) is illustrated in Figs. 12a–b. Here the balance winds are used to calculate zonal mean rms values of individual terms in the momentum equations [Eqs. (4a)–(4b)] and the respective rms residuals of the equations are also shown. The predominant geostrophic balance is clearly seen, along with

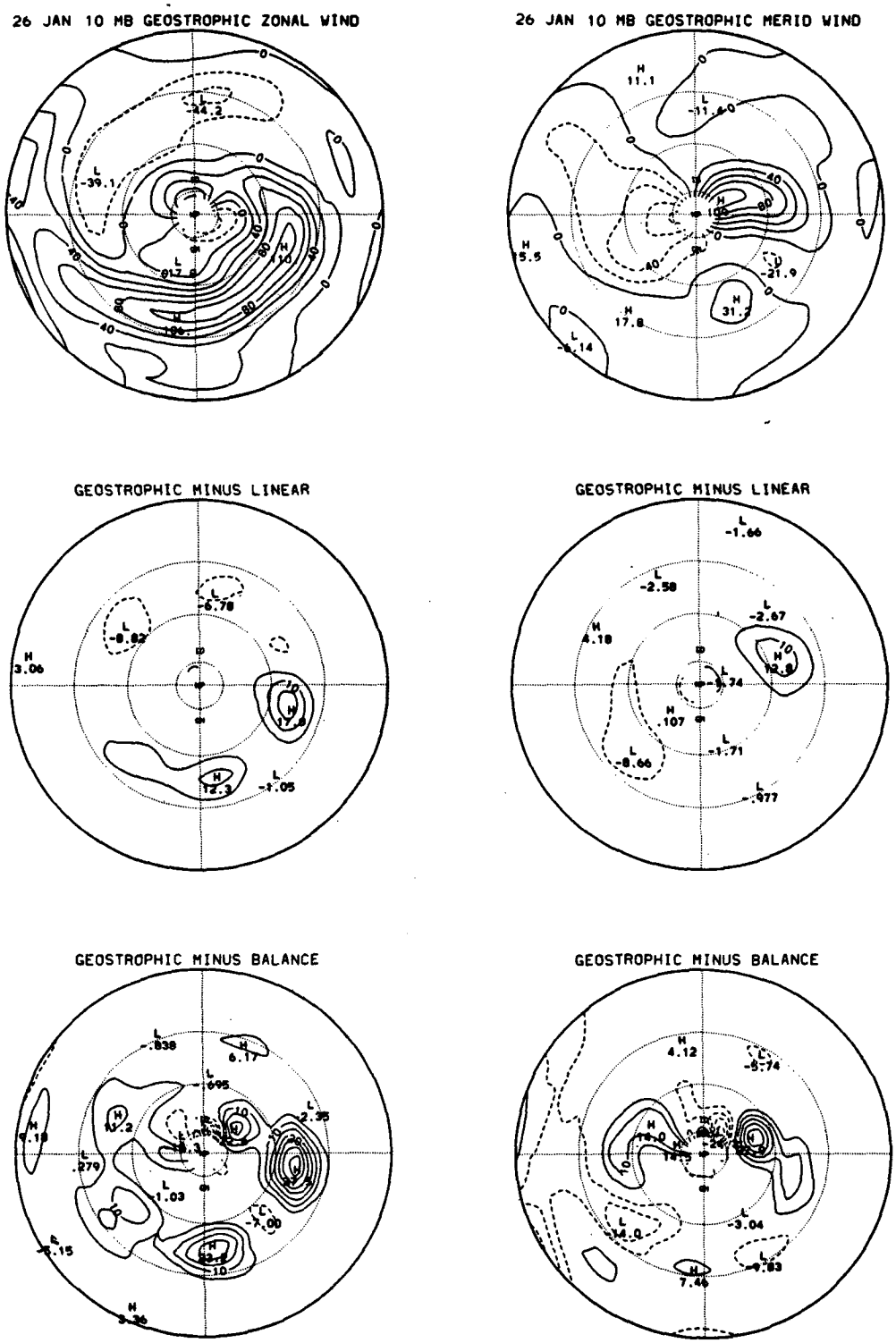

FIG. 11. NH polar stereographic plots of the 26 January 1979 geostrophic zonal and meridional winds (top), along with linear (middle) and balance (bottom) zonal and meridional winds plotted as differences from the geostrophic values. Units are m s^{-1}.

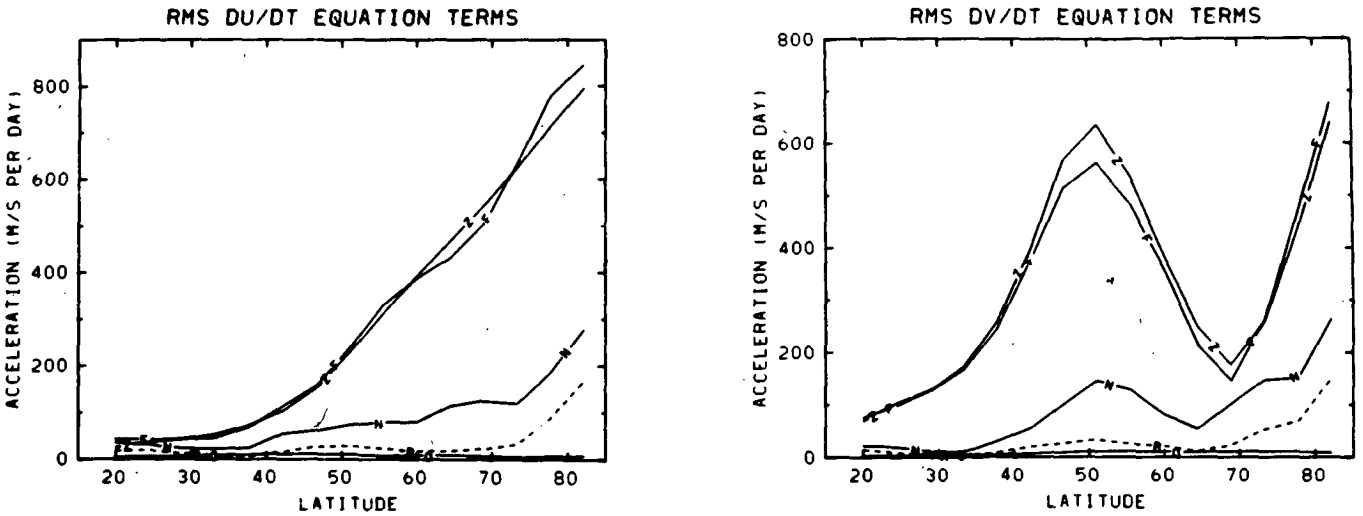

FIG. 12. Zonal mean rms values of different terms in the (left—Eq. 4a) zonal and (right—Eq. 4b) meridional momentum equations, plotted as a function of latitude, for 26 January 1979 at 10 mb. Calculations are based on balance winds. The lines are labeled as *Z*, geopotential gradient term; *F*, Coriolis term; *N*, nonlinear terms; *O*, observed time tendencies; and (dashed) *R*, equation residuals.

the relative importance of the nonlinear terms. The residuals in both equations are substantially smaller than the nonlinear terms, although they are markedly larger than the observed time tendencies (which were directly calculated from geostrophic winds and also plotted in Figs. 12a–b). These data are gridded via a Cressman-type analysis from all available observations within ±6 hours of 12 UTC, and therefore daily time tendencies cannot be accurately measured, particularly locally. Nonetheless, the observed small time tendency values suggest that neglect of these terms in (4a)–(4b) is a good assumption. The balances seen in Figs. 12a–b for 26 January at 10 mb are nearly identical to those for averages over longer periods during northern winter throughout 100 to 1 mb; even during times of intense wave growth the time tendency terms are observed to be much smaller than the nonlinear terms.

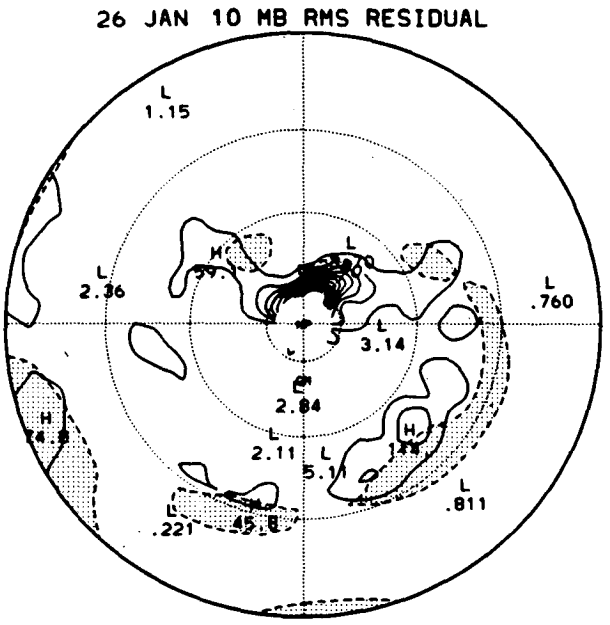

FIG. 13. NH polar stereographic projection of the square root of the sum of the squared residuals in the zonal and meridional momentum equations (Eqs. 4a–b), at 10 mb for 29 January 1979. Contour interval of 40 m s^{-1}/day. Also shown (as shaded regions) are areas where the nonlinear balance ellipticity criterion is violated (from Fig. 9b).

Inspection of local residuals from (4a)–(4b) (Fig. 13) shows that they are largest near the regions where the nonlinear balance ellipticity criterion is violated, i.e., where pure rotational winds cannot satisfy a balance relationship. Because observed local time tendencies are not large in these regions (note the caveat discussed above), the relatively large momentum equation residuals here suggest that the true balance in these areas must contain important contributions from either vertical advective terms or scales that are unresolved here.

Estimates of poleward momentum flux show geostrophic values larger than the other estimates by about 30% near 60°N. Poleward heat fluxes show smaller differences (order 10%) between the three estimates. Details of the flux comparisons are discussed for climatological means later.

An example of a strong wave event in the SH is discussed next. Figure 14 shows the 10 mb height on 29 August 1983, again the date of peak wave amplitude during a minor warming. In the SH winter, the polar vortex is much deeper, and the wave perturbations smaller than those observed in NH winters (cf. Fig.

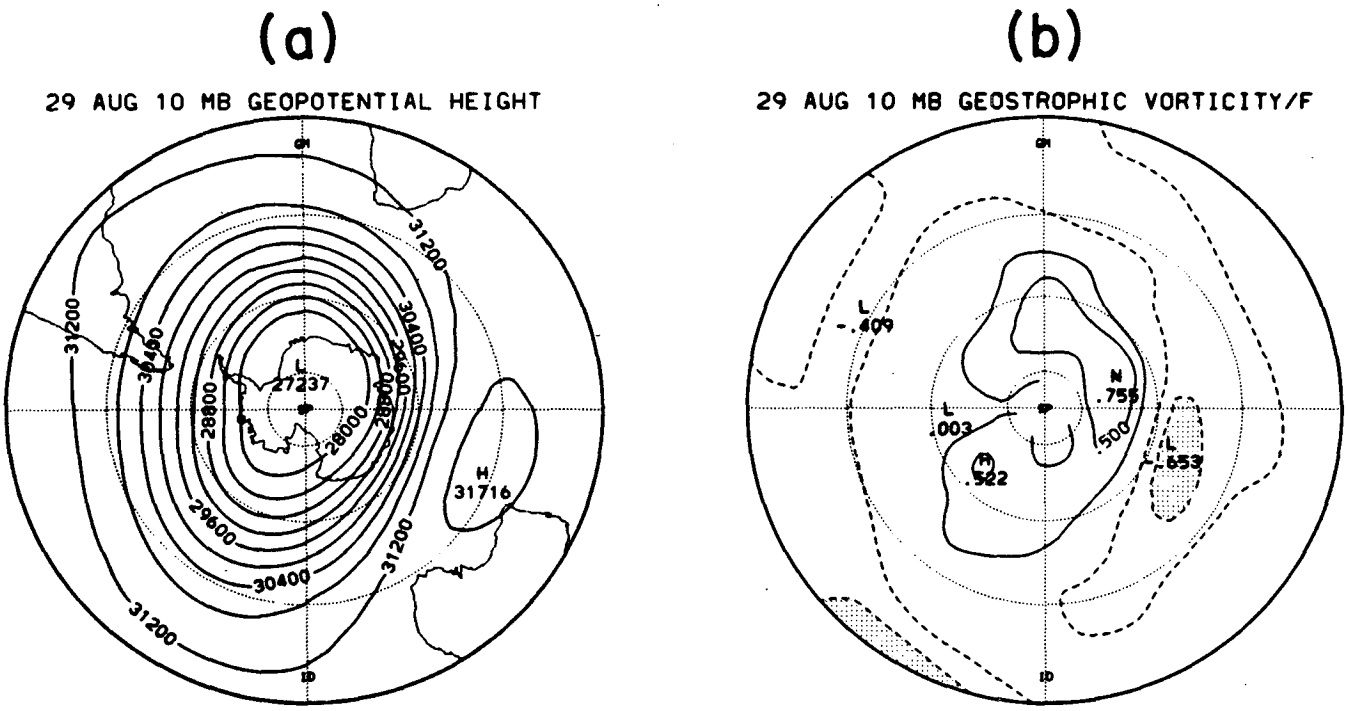

FIG. 14. As in Figs. 9a–b except for the SH case study, 29 August 1983.

9a). Figure 14b shows the quantity C [Eq. (9)]; in this case only a relatively small area exceeds the nonlinear balance ellipticity criterion ($C < -0.5$). Behavior of the iterative balance solution is shown in Fig. 10, with convergence being more rapid and systematic than for the NH examples.

Figure 15 shows the geostrophic zonal and meridional winds, along with the differences from geostrophy calculated using linear and balance estimates. Largest differences in the zonal winds are clearly in the regions of strong local curvature (cf. Fig. 14a); the linear and balance zonal wind estimates are in closer agreement than the NH example (Fig. 11) because the zonal mean flow is a better approximation to local values in the SH stratosphere.

A measure of local departure of linear or balance winds from geostrophic values in the SH winter is shown in Fig. 16a, where the zonal mean rms differences for both zonal and meridional wind components are shown for the month of August 1983. (Zonal means have been removed.) The linear and balance wind rms differences are similar, suggesting relatively little benefit is gained by the use of the full balance equations. (The rms differences between the linear and balance winds are 1–3 m s^{-1}.) In contrast, Fig. 16b shows similar statistics for January 1979; here the linear and balance winds show contrasting differences from geostrophy in low and high latitudes, and rms differences between the former are 3–6 ms. The large NH winter wave amplitudes lead to important *local* nonlinear terms that the balance technique can account for more accurately than the linear estimates (compare the linear and balance differences in Fig. 11). Statistics during spring in the SH (when wave activity is largest and the polar vortex is shallow) suggest a situation midway between these extremes.

Figure 17 displays zonal mean rms values of the separate momentum equation terms for the SH on 29 August. The same relative importance of terms is observed as for the NH case (Fig. 12), with the residuals quite a bit smaller than the nonlinear terms but larger than observed time tendencies. Local momentum equation residuals are shown in Fig. 18, exhibiting largest values near the region where pure rotational wind balance is prohibited, in striking similarity to the NH example (Fig. 13). Observed time tendencies are small in this region, again pointing to the possible importance of vertical advective terms or unresolved scales in the local momentum balance.

Figure 19a shows zonal mean rms values of relative vorticity evaluated with the different winds; here averages are taken over the month of August 1983 to be representative of typical active SH conditions. Geostrophic estimates are 10% larger than the linear and balance values. This agrees with the study of Clough et al. (1985), who state that using geostrophic winds results in roughly a 10% error in their calculations of isentropic potential vorticity. Also shown in Fig. 19a

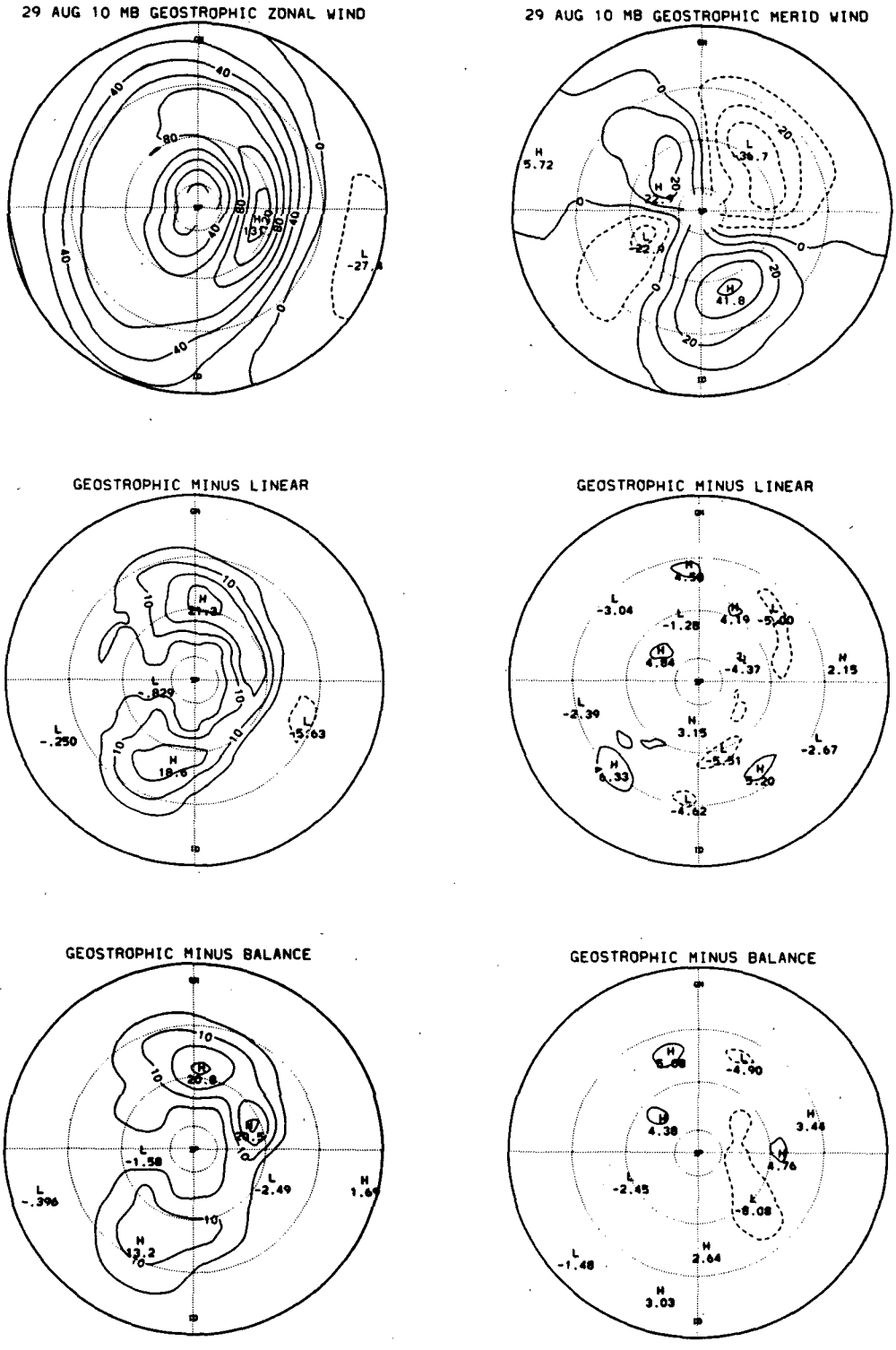

FIG. 15. As in Fig. 11 except for 29 August 1983.

are zonal mean rms values of the local horizontal divergence

$$D=\frac{1}{a\cos\phi}\left[\frac{\partial u}{\partial\lambda}+\frac{\partial}{\partial\phi}(v\cos\phi)\right],$$

estimated with the linear and balance winds. The ratio of divergence to vorticity is a measure of the importance of divergent versus rotational motion. The values seen in Fig. 19a show approximately an order of magnitude dominance of vorticity over divergence in the middle

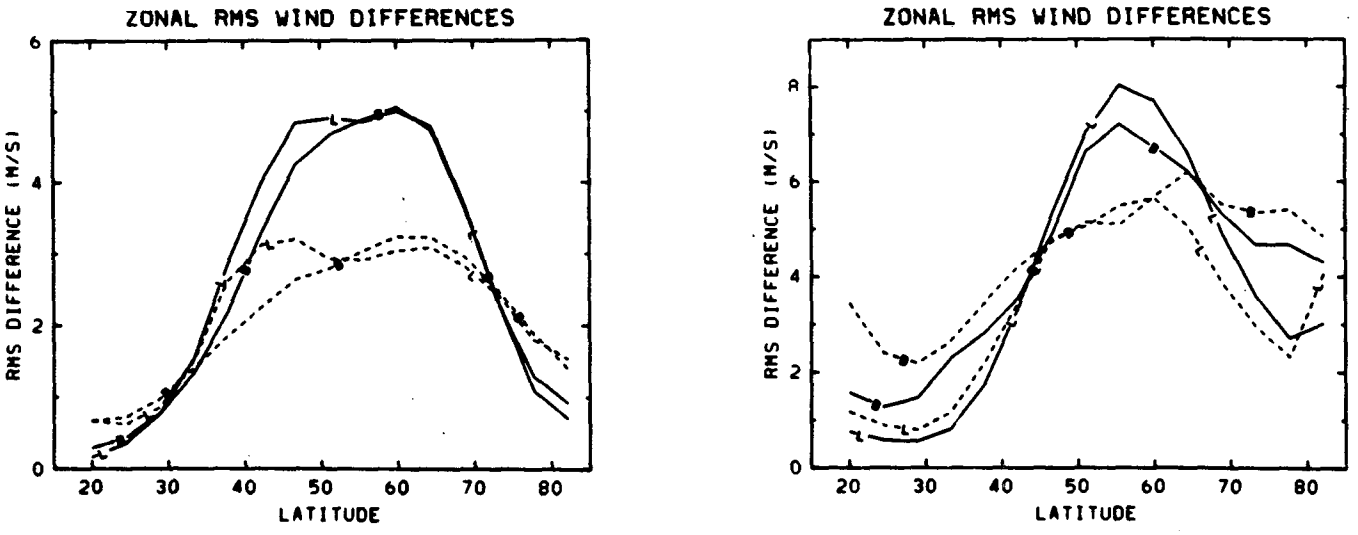

FIG. 16. 10 mb zonal mean rms differences between local geostrophic and (L) linear or (B) balance winds, for (solid) zonal and (dashed) meridional wind components. (a) SH average for August 1983, (b) NH average for January 1979. Note the different ordinate scales in (a)–(b).

stratosphere. Inspection of horizontal maps of the divergence estimates show that they are predominantly small scale (below the resolution retained in these analyses)—no planetary scale divergent patterns emerge other than that associated with the zonal mean meridional velocity. Similar behavior is observed at 1 mb.

Figure 19b shows similar calculations for the NH averaged over January 1979. Geostrophic rms zonal mean vorticity values are only slightly larger than linear or balance estimates. The ratio of rms vorticity to divergence shows approximately a factor of 5 or larger dominance of vorticity in the middle stratosphere; similar behavior is observed at 1 mb.

The geostrophically evaluated poleward momentum flux in the SH is found to be an overestimate by about 60% near 60°S. Geostrophic winds consistently overestimate poleward momentum fluxes because in cyclonic flow the geostrophic wind is always an overestimate of the balance wind; both zonal and meridional components are affected near regions of strong curvature, and the individual errors are compounded when their product is calculated. Larger relative errors are found in the SH because of the stronger polar night jet and the larger associated centrifugal accelerations. Poleward heat flux values exhibit relatively small differences from geostrophy; this shows a lack of consistent zonal correlation between the ageostrophic me-

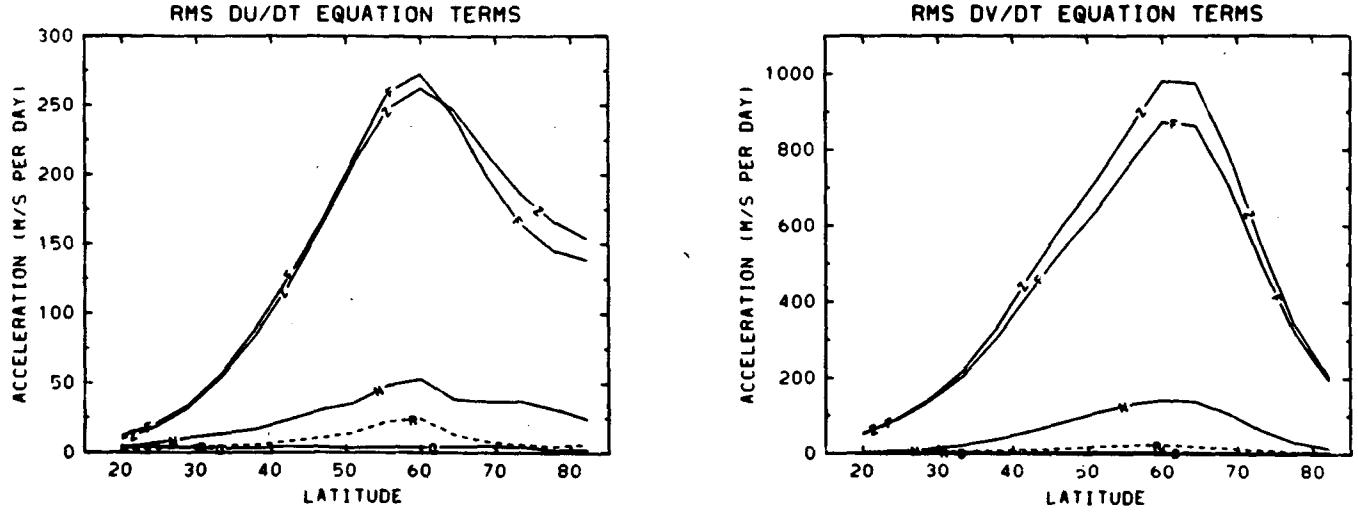

FIG. 17. As in Fig. 12 except for 10 mb in the SH for 29 August 1983.

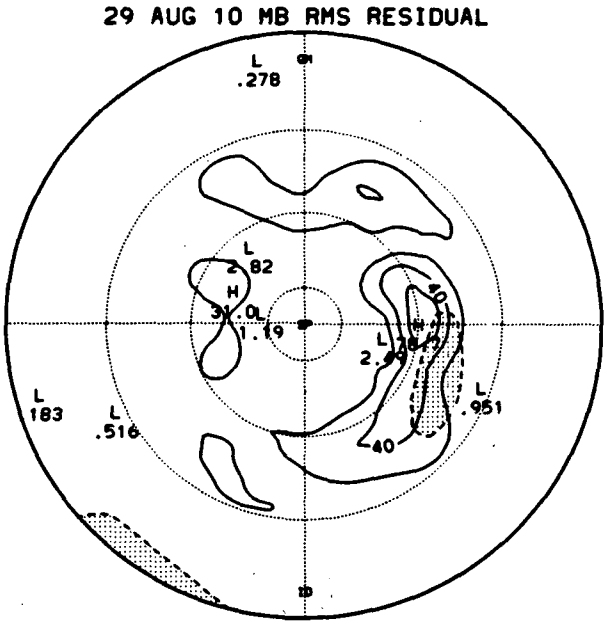

FIG. 18. As in Fig. 13 except for 10 mb in the SH for 29 August 1983. The shaded region is from Fig. 14b.

ridional wind and temperature fields. Details for climatological means are discussed below.

b. *Climatological analyses*

Climatological wind analyses are presented in this section for averages over seven years (1979–85) of January (NH) and August (SH) data. Figures 20a–c show the January average zonal mean zonal wind evaluated using geostrophic, gradient, and balance estimates. The balance and gradient values are nearly identical, while geostrophic zonal mean winds are overestimates by 10%–15% near the core of the polar night jet. The balance zonal mean meridional winds (Fig. 20d) show poleward flow in the low-latitude stratosphere and equatorward flow in high latitudes, implying convergence near 45°N. Mean meridional velocities are on the order of 1 m s^{-1} in the upper stratosphere.

Figure 21 shows the poleward momentum and heat fluxes evaluated with geostrophic and balance winds, and their differences. Because linear wind estimates of the momentum and heat fluxes are nearly identical to the balance wind values, only the balance wind fluxes are displayed. Geostrophic momentum fluxes in Fig. 21 are systematically larger than balance values in the high-latitude stratosphere by as much as 40%. Heat flux estimates are similar between the methods, with geostrophic values being only 5%–10% larger than the balance fluxes, primarily poleward of the jet core.

Figure 22 compares EP flux divergence estimates based on the different wind analyses; here the linear wind estimate is also included. Geostrophic wind values show excessive convergence in midlatitudes and reduced convergence–positive divergence in the high-latitude stratosphere, resulting from the geostrophic overestimate of poleward momentum flux (Fig. 21). The linear and balance estimates show convergence of the EP flux throughout most of the stratosphere, with strongest values in the middle to upper stratosphere polewards of 55°N, and in the subtropical upper stratosphere near 35°N.

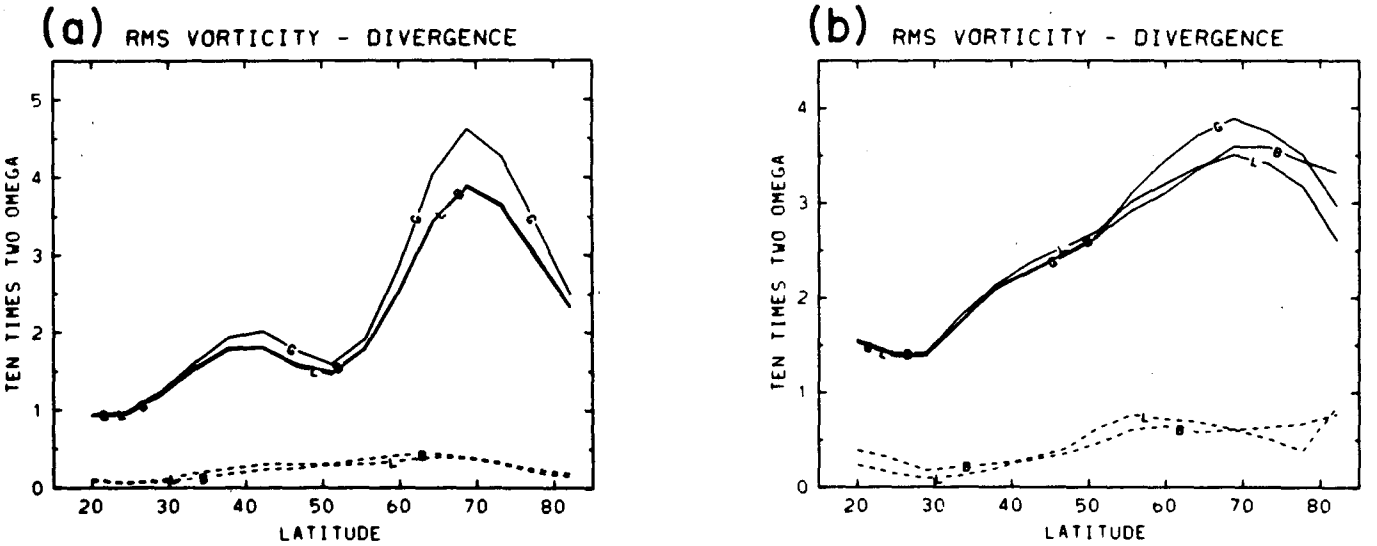

FIG. 19. (a) 10 mb zonal mean rms relative vorticity estimates from (G) geostrophic, (L) linear, and (B) balance winds (solid lines), along with zonal mean rms divergence estimates from (L) linear and (B) balance winds (dashed lines), for the SH averaged over August 1983. Units are $10 \times 2\Omega = 1.46 \times 10^{-4}$ s^{-1}. (b) As in (a) except for the NH averaged over January 1979.

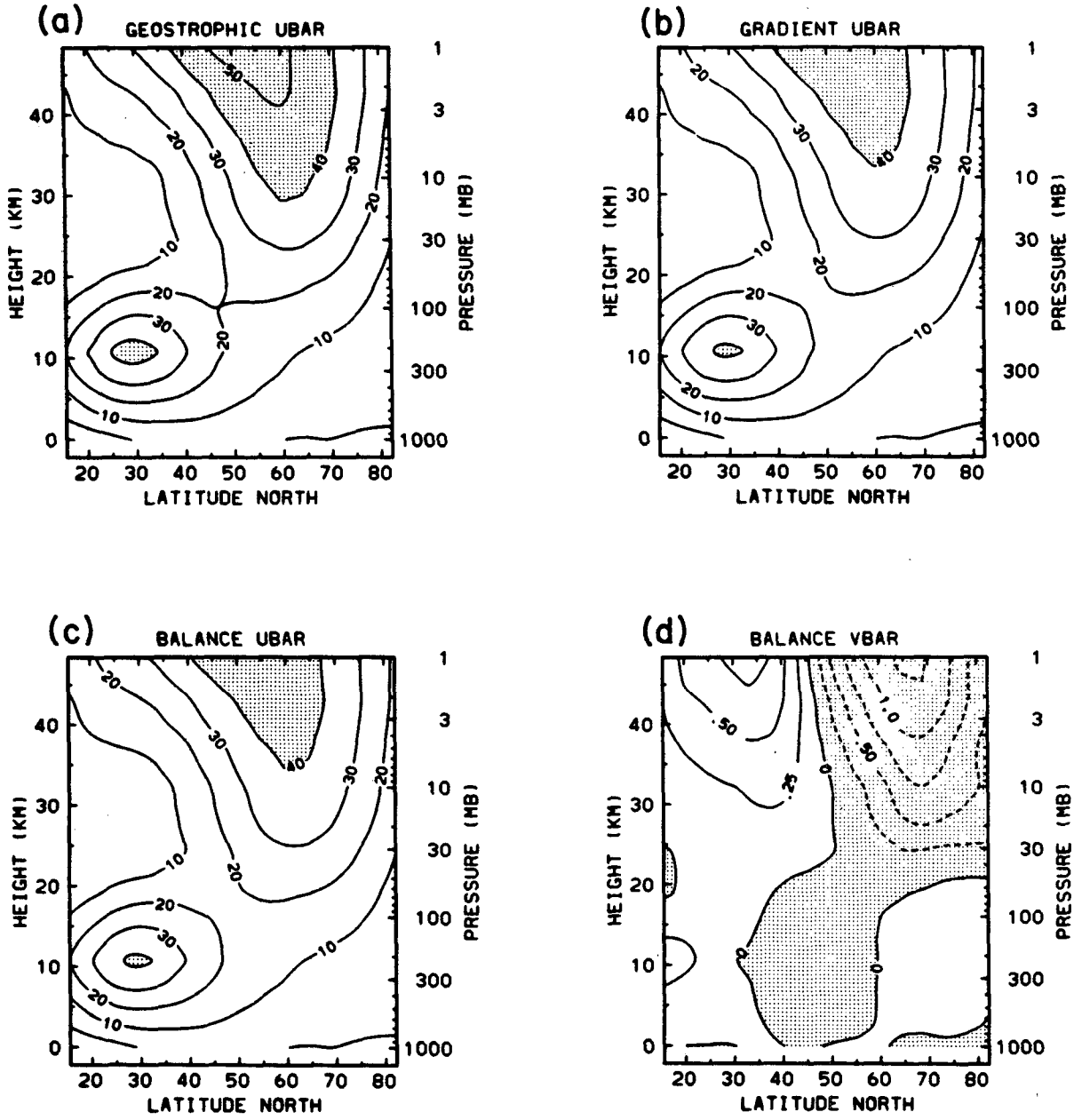

FIG. 20. Zonal mean zonal wind for NH January climatology (1979–85), evaluated using (a) geostrophic, (b) gradient, and (c) balance winds. Units are m s^{-1}. Zonal mean balance meridional wind is shown in (d), with contour interval of 0.25 m s^{-1}.

Figures 23a–c show the August average zonal mean zonal wind estimates. The balance and gradient values show excellent agreement, whereas the geostrophic values are more than 10 m s^{-1} too large near the polar night jet core. The balance zonal mean meridional wind (Fig. 23d) exhibits the same two-cell structure found in the NH (Fig. 20d), with the magnitudes reduced by nearly a factor of 2.

Comparison of the geostrophic and balance momentum fluxes (Fig. 24) shows large relative geostrophic errors in the high-latitude stratosphere; geostrophic values are nearly a factor of 2 too large near 65°–70°S. This larger relative difference (compared to the NH) results from the stronger SH polar night jet. The geostrophic and balance heat flux estimates show a 10%–15% geostrophic overestimate in the lower stratosphere, with smaller relative differences above.

The geostrophic wind EP flux divergence estimate in Fig. 25 shows a strong north–south dipole pattern in the middle and upper stratosphere. Comparison with

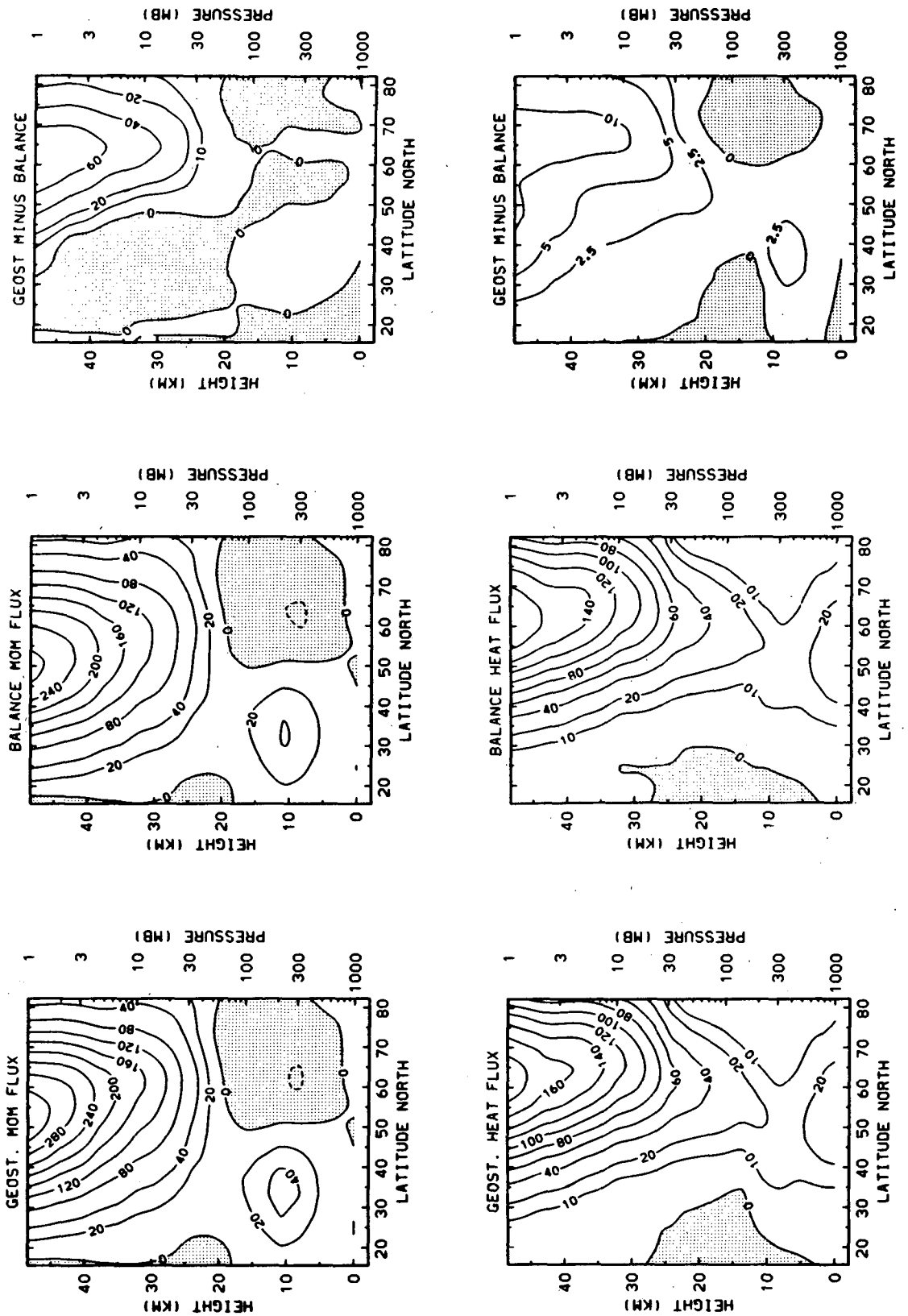

FIG. 21. (top) Poleward momentum flux for NH January climatology evaluated using (left) geostrophic winds, (middle) balance winds, and (right) their difference. Units of $m^2 s^{-2}$. (bottom) As above, except for poleward heat flux estimates. Units of degrees K–m s^{-1}.

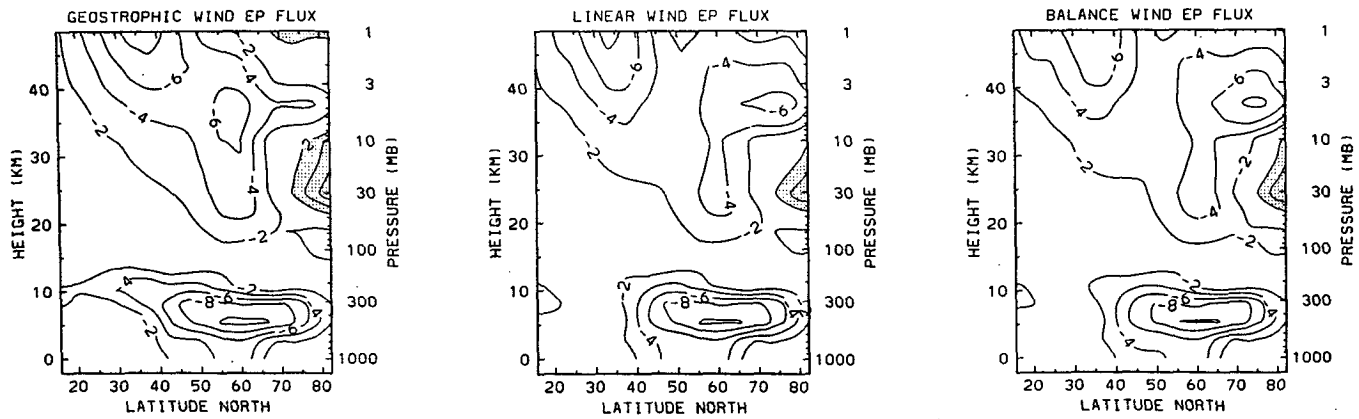

FIG. 22. EP flux divergence estimates for NH January climatology, based on (left) geostrophic, (middle) linear, and (right) balance wind heat and momentum fluxes. Units of wave driving are m s^{-1}/day. Zero contours are omitted, and positive regions are shaded.

the linear and balance estimates show that the positive divergence feature in the middle stratosphere results primarily from the use of geostrophic wind fluxes. The strongest EP flux convergence is observed in the subtropical upper stratosphere near 35°–40°S, very similar to the NH January maximum in Fig. 22 (although reduced in magnitude by 30%–50%). The NH statistics also show significantly stronger wave driving in the troposphere.

6. Summary

This work has focused on evaluating stratospheric wind fields from geopotential height data alone, with emphasis on improvement over local geostrophic estimates. Several methods of maintaining higher-order balance between the wind and height fields have been analyzed. Solution of the nonlinear balance equation was tested and found to be frequently insolvable due to violation of ellipticity constraints, particularly when strong planetary waves are present in the stratosphere. This problem is more acute in the NH winter stratosphere and renders an unsatisfactory verdict on the practical use of this method. Linear balance winds are not substantially different from local geostrophic values.

A new method tested here of maintaining higher-order balance is the iterative solution of the coupled zonal and meridional momentum equations, minus the time tendency and vertical advection terms (yielding "balance" winds). Rapid convergence of these equations is usually observed, with relative differences dropping to 5%–10% after 2–3 iterations. Observed small residuals of the equations show that accurate balance is achieved. Additionally, the time tendency terms are measured observationally and shown to be negligible. A third wind analysis method tested was the use of momentum equations linearized about the zonal mean wind, as suggested by Robinson (1986), resulting in so-called "linear" winds.

The geostrophic, linear, and balance wind estimates are compared with actual stratospheric winds resulting from a general circulation model simulation of the NH troposphere and stratosphere; additionally, the three estimates are compared with each other for observational data, both for case studies and for NH and SH climatologies. These comparisons yield the following net results:

(i) Geostrophic zonal mean zonal winds substantially overestimate the strength of the stratospheric polar night jet, as noted in many previous studies (e.g., Quiroz, 1981; Boville, 1987). Balance zonal mean zonal winds yield the most accurate estimates, but in practice nearly as much accuracy can be obtained for all but the most active periods from gradient zonal mean winds (Eq. 7), which are substantially easier to calculate. The balance solutions also yield zonal mean meridional winds; these show good agreement with the model statistics in middle to high latitudes.

(ii) Estimates of poleward momentum fluxes are severely biased in the high-latitude stratosphere by geostrophic winds. This is primarily due to the lack of centrifugal terms in the geostrophic equations and the positive correlation between ageostrophic zonal and meridional winds in regions of strong curvature. Larger relative errors are observed in the SH winter, due to the stronger polar night jet intensity. The use of linear or balance winds in the flux calculations substantially alleviates this problem; both calculations show near identical results.

Poleward heat flux estimates are not substantially different in the observational data between the three wind estimates. (Geostrophic values are approximately 10% larger than linear or balance fluxes.) The model comparisons show a substantial geostrophic error that

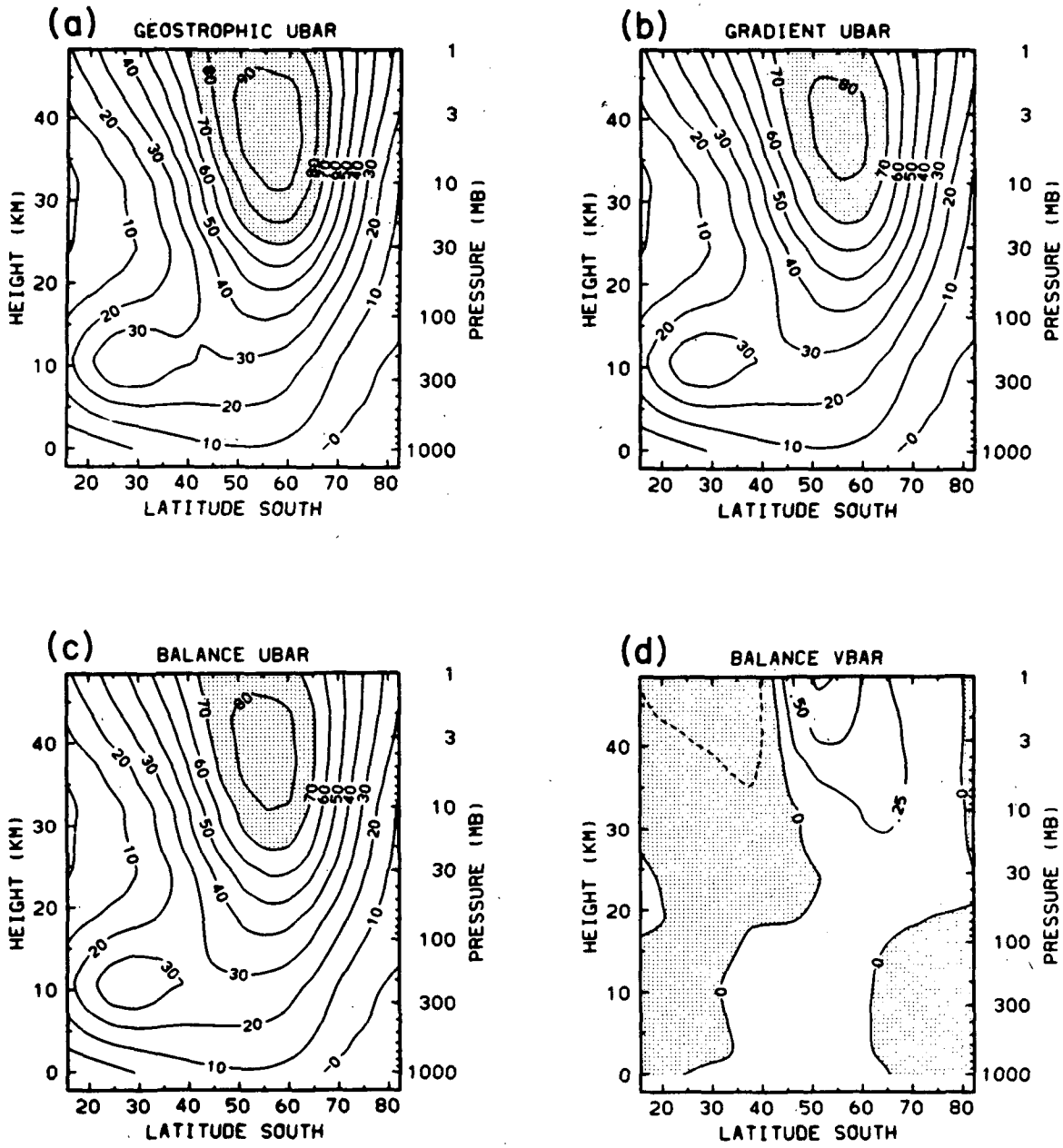

FIG. 23. As in Fig. 20 except for SH August climatology (1979–85).

is probably related to the excessively strong stationary waves in the model.

Geostrophic wind EP flux calculations show substantial errors in the high-latitude stratosphere, resulting primarily from the geostrophic overestimates of poleward momentum flux. Values based on balance or linear wind fluxes give superior results. Overall, the balance and linear wind heat, momentum, and EP fluxes show near identical results. Because the linear winds are substantially easier to calculate, they may be preferable when only flux quantities are needed.

(iii) Comparison of *local* model winds with the three estimates gives a clear advantage to the balance winds. Although no similar comparisons have been made for observed winds, the balance winds are felt to be the superior analysis technique for evaluating local winds in the NH. Linear and balance winds yield similar local values in the SH winter, where the linear approximation is more valid. Local balance values may be superior during transition seasons in the SH.

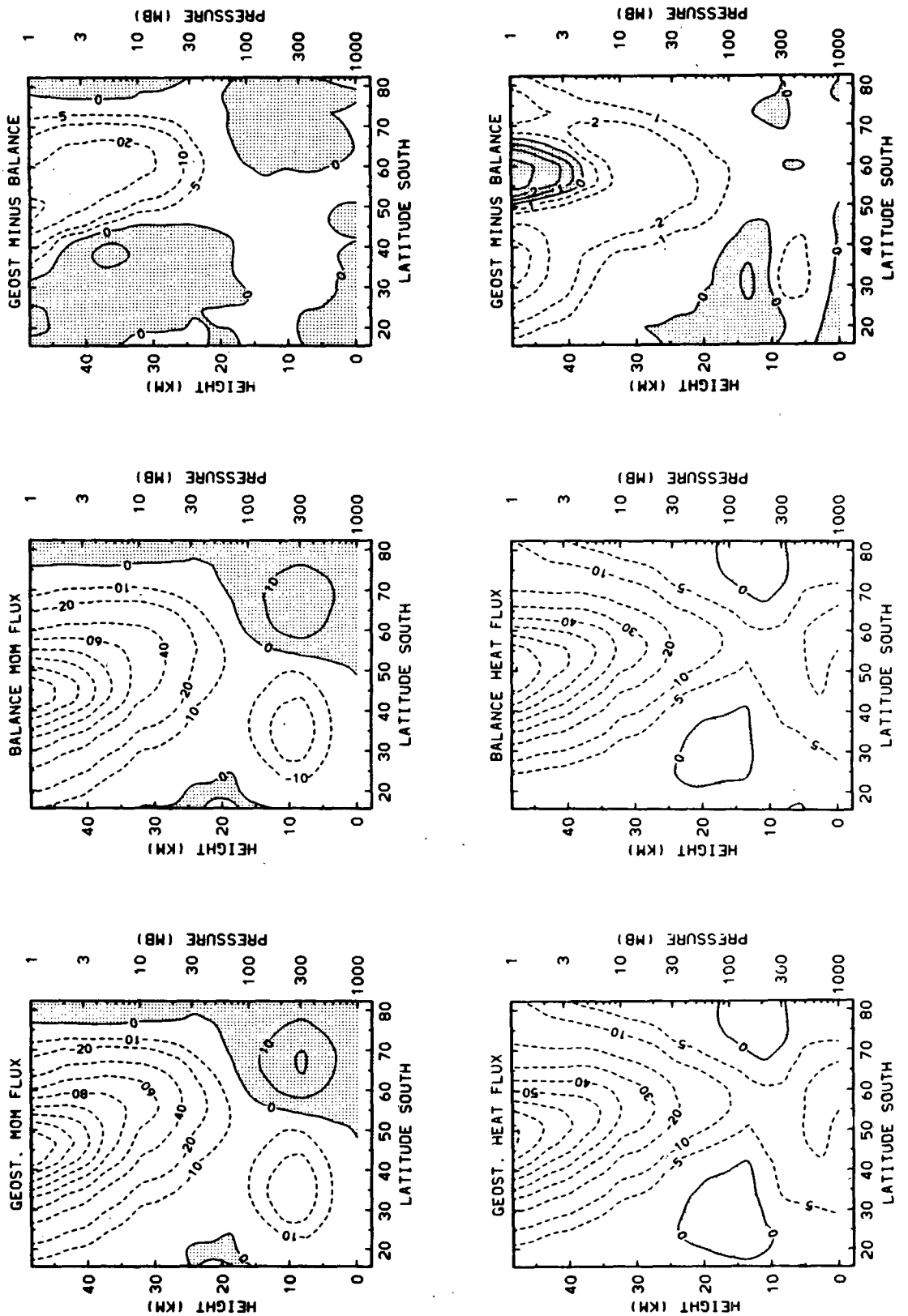

FIG. 24. As in Fig. 21 except for SH August climatology (1979–85).

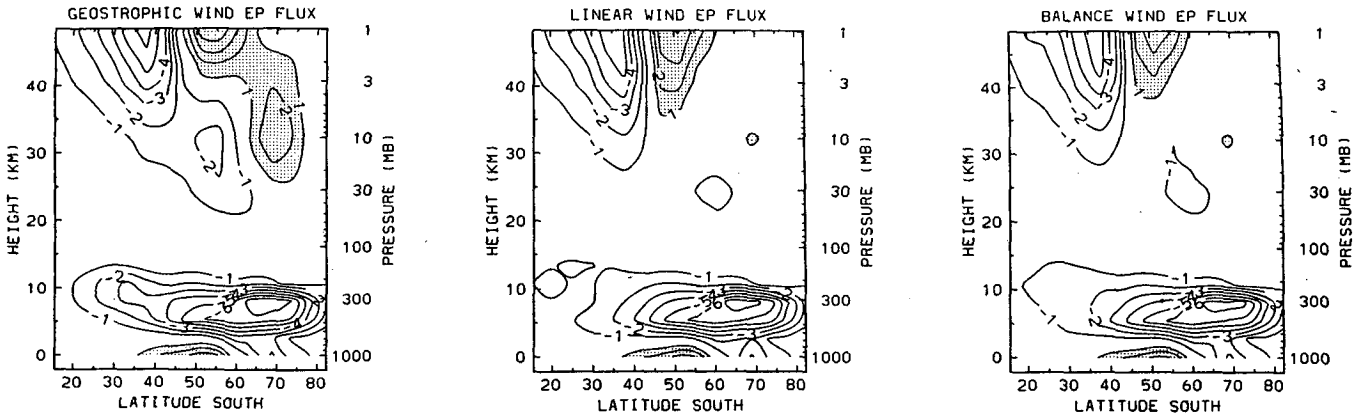

FIG. 25. As in Fig. 22 except for SH August climatology (1979–85). Contour interval of 1 m s^{-1} per day.

Estimates of the relative importance of rotational versus divergent motions in the stratosphere have been made for NH and SH observational data, based on the zonal mean rms relative vorticity and divergence fields calculated with the linear and balance winds. The rms relative vorticities are typically five to ten times larger than the rms divergence values, illustrating a decisive dominance of rotational motion. Relatively larger momentum equation residuals are observed near areas where the nonlinear balance ellipticity constraint is violated (and thus no pure rotational wind balance is possible). Because observed time tendencies are small, this suggests that vertical advective terms or motion at unresolved scales may be important to the local momentum balances in these regions.

Acknowledgments. The author wishes to thank Byron Boville for sharing his model results and data analysis routines. He also, along with Peter Gent and Joseph Tribbia, provided insightful discussions throughout the course of this work. Numerous colleagues provided valuable comments on an earlier version of this manuscript.

REFERENCES

Boville, B. A., 1987: The validity of the geostrophic approximation in the winter stratosphere and troposphere. *J. Atmos. Sci.*, **44**, 443–457.

——, and W. J. Randel, 1986: Observations and simulation of the variability of the stratosphere and troposphere in January. *J. Atmos. Sci.*, **43**, 3015–3034.

Burger, A. P., 1958: Scale consideration of planetary motion of the atmosphere. *Tellus*, **10**, 205–205.

Charney, J. G., 1955: The use of the primitive equations of motion in numerical prediction. *Tellus*, **7**, 22–26.

Clough, S. A., N. S. Graham and A. O'Neill, 1985: Potential vorticity in the stratosphere derived using data from satellites. *Quart. J. Roy. Meteor. Soc.*, **111**, 335–358.

Dunkerton, T., C.-P. F. Hsu and M. E. McIntyre, 1981: Some Eulerian and Lagrangian diagnostics for a model stratospheric warming. *J. Atmos. Sci.*, **38**, 819–843.

Elson, L. E., 1986: Ageostrophic motions in the stratosphere from satellite observations. *J. Atmos. Sci.*, **43**, 409–418.

Geller, M. A., M.-F. Wu and M. E. Gelman, 1983: Troposphere–stratosphere (surface—55 km) monthly winter general circulation statistics for the Northern Hemisphere—four year averages. *J. Atmos. Sci.*, **40**, 1334–1352.

——, —— and ——, 1984: Troposphere–stratosphere (surface—55 km) monthly winter general circulation statistics for the Northern Hemisphere—interannual variations. *J. Atmos. Sci.*, **41**, 1726–1744.

Gent, P. R., and J. C. McWilliams, 1983: Regimes of validity for balanced models. *Dyn. Atmos. Ocean*, **7**, 167–183.

Haltiner, G. J., and R. T. Williams, 1980: *Numerical Prediction and Dynamic Meteorology*, 2nd ed., Wiley and Sons, 477 pp.

Hartmann, D. L., C. R. Mechoso and K. Yamazaki, 1984: Observations of wave-mean flow interaction in the Southern Hemisphere. *J. Atmos. Sci.*, **41**, 351–362.

Hitchman, M. H., C. B. Leovy, J. C. Gille and P. L. Bailey, 1987: Quasi-stationary zonally asymmetric circulations in the equatorial lower mesosphere. *J. Atmos. Sci.*, **44**, 2119–2136.

Holton, J. R., 1979: *An Introduction to Dynamic Meteorology*, 2nd ed., Academic Press, 391 pp.

Mechoso, C. R., D. L. Hartmann and J. D. Farrara, 1985: Climatology and interannual variability of wave mean-flow interaction in the Southern Hemisphere. *J. Atmos. Sci.*, **42**, 2189–2206.

Phillips, N. A., 1963: Geostrophic motion. *Reviews of Geosphysics*, **1**, 123–176.

Quiroz, R. S., 1981: The tropospheric–stratospheric mean zonal flow in winter. *J. Geophys. Res.*, **86**, 7378–7384.

Robinson, W. A., 1986: The application of the quasi-geostrophic Eliassen–Palm flux to the analysis of stratospheric data. *J. Atmos. Sci.*, **43**, 1017–1023.

Smith, A. K., 1984: Comparison of winds derived from the LIMS satellite instrument with rocket observations. NCAR Tech. Note NCAR/TN-325+STR, 81 pp.

Trenberth, K. E., 1987: The role of eddies in maintaining the westerlies in the Southern Hemisphere winter. *J. Atmos. Sci.*, **44**, 1498–1508.

Tribbia, J. J., 1981: Nonlinear normal-mode balancing and the ellipticity condition. *Mon. Wea. Rev.*, **109**, 1751–1761.